การปรับปรุงความว่องไวของตัวเร่งปฏิกิริยาทางไฟฟ้าเคมีที่ไม่เป็นไปตามกฎของฟาราเดย์ของการออกซิเดชันโพรเพนบนอิตเทรียสเตบิไลซ์เซอร์โคเนียที่เคลือบฝังด้วยแพลตินัม

นางสาวโสภาวรรณ ยินดี

วิทยานิพนธ์นี้เป็นส่วนหนึ่งของการศึกษาตามหลักสูตรปริญญาวิศวกรรมศาสตรมหาบัณฑิต
สาขาวิชาวิศวกรรมเคมี ภาควิชาวิศวกรรมเคมี
คณะวิศวกรรมศาสตร์ จุฬาลงกรณ์มหาวิทยาลัย
ปีการศึกษา 2558

Non-faradaic electrochemical modification of catalytic activity of propane oxidation on Pt-impregnated YSZ

Miss Sopawan Yindee

A Thesis Submitted in Partial Fulfillment of the Requirements
for the Degree of Master of Engineering Program in Chemical Engineering
Department of Chemical Engineering
Faculty of Engineering
Chulalongkorn University
Academic Year 2015

Thesis Title	Non-faradaic electrochemical modification of catalytic activity of propane oxidation on Pt-impregnated YSZ
By	Miss Sopawan Yindee
Field of Study	Chemical Engineering
Thesis Advisor	Palang Bumroongsakulsawat, Ph.D.

Accepted by the Faculty of Engineering, Chulalongkorn University in Partial Fulfillment of the Requirements for the Master's Degree

.....Dean of the Faculty of Engineering
(Associate Professor Supot Teachavorasinskun, D.Eng.)

THESIS COMMITTEE

.....Chairman
(Professor Suttichai Assabumrungrat, Ph.D.)

.....Thesis Advisor
(Palang Bumroongsakulsawat, Ph.D.)

.....Examiner
(Assistant Professor Apinan Soottitantawat, Ph.D.)

.....External Examiner
(Assistant Professor Worapon Kiatkittipong, Ph.D.)

โสภาวรรณ ยินดี : การปรับปรุงความว่องไวของตัวเร่งปฏิกิริยาทางไฟฟ้าเคมีที่ไม่เป็นไปตามกฎของฟาราเดย์ของการออกซิเดชันโพรเพนบนอิตเทรียสเตบิไลซ์เซอร์โคเนียที่เคลือบฝังด้วยแพลตินัม (Non-faradaic electrochemical modification of catalytic activity of propane oxidation on Pt-impregnated YSZ) อ.ที่ปรึกษาวิทยานิพนธ์หลัก: ดร. พลัง บำรุงสกุลสวัสดิ์, 4 หน้า.

งานวิจัยนี้เปรียบเทียบผลของวิธีเตรียมตัวเร่งปฏิกิริยาแพลตินัมบนอิตเทรียสเตบิไลซ์เซอร์โคเนียต่อการปรับปรุงความว่องไวของตัวเร่งปฏิกิริยาทางไฟฟ้าเคมีที่ไม่เป็นไปตามกฎของฟาราเดย์ โดยใช้ปฏิกิริยาโพรเพนออกซิเดชันเป็นปฏิกิริยาต้นแบบ ตัวเร่งปฏิกิริยาถูกเตรียมขึ้นสองวิธีด้วยการดูดซับแบบไฟฟ้าสถิตย์อย่างแรงและการเคลือบฝังแบบเปียก โดยปริมาณแพลตินัมที่อยู่บนตัวรองรับต่อพื้นที่ผิวถูกกำหนดให้เท่ากันในทั้งสองวิธี การปรับปรุงความว่องไวของตัวเร่งปฏิกิริยาทางไฟฟ้าเคมีที่ไม่เป็นไปตามกฎของฟาราเดย์ของปฏิกิริยาโพรเพนออกซิเดชันถูกศึกษาภายใต้สภาวะออกซิเจนพอดีที่อุณหภูมิ 200-480 องศาเซลเซียส ความดันบรรยากาศ และช่วงความต่างศักดิ์ทางไฟฟ้า 6-30 โวลต์ เมื่อทำปฏิกิริยาที่อุณหภูมิ 200 องศาเซลเซียสและความต่างศักย์ไฟฟ้า 6 โวลต์ จะได้ค่าผลได้ฟาราเดย์สูงสุดซึ่งมีค่าเท่ากับ 5.2×10^4 ด้วยตัวเร่งปฏิกิริยาที่ถูกสังเคราะห์โดยวิธีการดูดซับแบบไฟฟ้าสถิตย์อย่างแรง อย่างไรก็ตามค่าผลได้ฟาราเดย์ลงลดเมื่ออุณหมิที่ใช้ทำปฏิกิริยาเพิ่มขึ้น ผลการวิเคราะห์การกระจายตัวของโลหะด้วยวิธีการดูดซับก๊าซคาร์บอนมอนออกไซด์แสดงให้เห็นว่าค่าการกระจายตัวของวิธีการดูดซับแบบไฟฟ้าสถิตย์อย่างแรงมีค่า 80.79% ซึ่งสูงกว่าค่าของวิธีการเคลือบฝังแบบเปียกที่ 44.34%

ภาควิชา วิศวกรรมเคมี ลายมือชื่อนิสิต .....

สาขาวิชา วิศวกรรมเคมี ลายมือชื่อ อ.ที่ปรึกษาหลัก .....

ปีการศึกษา 2558

5770346721 : MAJOR CHEMICAL ENGINEERING

KEYWORDS: NEMCA, PROPANE OXIDATION, PT-YSZ, IMPREGNATION, SEA

SOPAWAN YINDEE: Non-faradaic electrochemical modification of catalytic activity of propane oxidation on Pt-impregnated YSZ. ADVISOR: PALANG BUMROONGSAKULSAWAT, Ph.D., 4 pp.

Effects of two Pt-YSZ fabrication methods on Non-Electrochemical Modification of Catalytic Activity (NEMCA) of propane oxidation were studied. Pt-YSZ were prepared either by strong electrostatic adsorption (SEA) or by wet impregnation (WI), for both of which the Pt loadings on YSZ were equal. NEMCA of propane oxidation at the prepared supported catalyst was studied under a stoichiometric amount of oxygen at 200-480 °C, atmospheric pressure, and in a range of electrical potential of 6-30 V. The highest faradaic yield of 5.2×10^4 was achieved at 200 °C with a cell voltage of 6 V at Pt-YSZ prepared by SEA. However, the faradaic yields decreased as the temperature was increased. The dispersion of Pt of the supported catalysts was characterized by CO chemisorption. The results indicated that SEA offered higher Pt dispersion of 80.79%, compared to the value from WI at 44.34%.

Department: Chemical Engineering Student's Signature .....

Field of Study: Chemical Engineering Advisor's Signature .....

Academic Year: 2015

ACKNOWLEDGEMENTS

First of all, the author would like to express her greatest thankfulness and appreciation to her adviser, Dr. Palang Bumroongsakulsawat for his instruction and valuable suggestions throughout this research. Without his guidance and persistent help this thesis would not have been possible. The author would also be grateful to Professor Suttuchai Assabumrungrat, Ph.D., as the Chairman, Assistant Professor Apinan Soottitantawat, and Assistant Professor Worapon Kiatkittipong as members of the thesis committer.

Moreover, the author would like to thank all those who have helped, supported and encouraged in this research, especially research assistants, all my friends and my parents.

In addition, this research was financially support to this work under The Institutional Research Grant and Chulalongkorn University (The Thailand Research Fund)

CONTENTS

Page

Page

Page

TABLES CONTENT

Page

FIGURES CONTENT

Page

CHAPTER I
INTRODUCTION

1.1 Background

The catalytic oxidation of hydrocarbons has received great attention from many researchers since it provides a more environmentally friendly alternative to conventional combustion by flame. Pt is considered the most active metal for the oxidation of hydrocarbons [1, 2] and thus has been incorporated in catalytic converters for the oxidation of residual light hydrocarbons. Nowadays, vehicles with internal combustion engines have become necessities for every household. Therefore, more catalytic converters are needed, while the rising price of the precious metal calls for more efficient use of the catalyst.

Non-faradaic Electrochemical Modification of Catalytic Activity (NEMCA), or Electrochemical promotion of catalysis (EPOC) is a process by which when electrical potential differences are imposed on two catalyst electrodes separated by an electrolyte, the catalytic rate of the formation of a product at one or more of the catalysts is enhanced above that which could possibly be attained were the reaction purely electrochemical. This phenomenon allows in situ and reversible tuning of catalytic performance by applying externally a potential or current between two electrodes [3]. Catalyst, counter, and reference electrodes are deposited on a solid electrolyte, i.e. yttria-stabilized zirconia (YSZ). As one of the electrode is positively biased, the electrochemically generated O^{2-} species migrate through the solid electrolyte to that electrode at a rate of I/2F. This causes changes in the electronic properties of the surface that alter the chemisorptive and catalytic properties of the catalyst-electrode [3, 4]. Increased catalytic oxidation rates of hydrocarbons through this phenomenon could shorten the lengths of catalytic converters and reduce the amounts of catalysts.

Electrodes for NEMCA studies are conventionally fabricated with platinum paste [1, 5] or by sputtering [3, 6, 7], which require considerably large amounts of the

metal catalyst and provide thick platinum layers. Since the size of platinum particles prepared by these two methods are in micron range, a significant portion of the catalyst is inactive and serve only as electrical connectors. Therefore, these deposition methods are impractical for commercial implementation.

One of the simplest methods for preparing metal-supported catalysts is Strong Electrostatic Adsorption (SEA). This method is a special case of wet impregnation (WI), by which the final pH of the precursor solution is set to the pH that yields the strongest electrostatic interaction between the metal ions in the solution and the support. SEA also allows platinum to form highly dispersed nanoparticles [8] and could be easily applied to solid electrolytes in disk shapes. This led to this study of NEMCA at platinum deposited on YSZ prepared by SEA in comparison with that prepared by conventional wet impregnation.

1.2 Research objectives

1. To find suitable conditions for the deposition of Pt at YSZ by SEA.
2. To study and compare the dependence of propane oxidation rates on applied potentials and temperatures at Pt-YSZ prepared by SEA and WI.

1.3 Research scopes

1. Effects of potential differences up to 30 volts on reaction rates
2. Effects of the temperature within 200-480 ^{o}C on reaction rates
3. Pt-YSZ prepared by SEA and WI

CHAPTER II
THEORY

In this research is based on theory of impregnation, Strong electrostatic adsorption (SEA), Non-Faradaic Electrochemical Modification of Catalytic Activity (NEMCA), and some information about platinum and Yttria-stabillized zirconia (YSZ).

2.1 Impregnation

Impregnation is a commonly used technique for the synthesis of heterogeneous catalysts. It is achieved by firstly filling the pores of a support with a solution of the metal salt. The solvent is then removed mostly by evaporation. Eventually, the desired metal is obtained by thermal decomposition and/or reduction. With this method of preparation, it is necessary to have an understanding of both chemical and physical properties of the support and the chemistry of the impregnating solution in order to control the physical properties of the finished catalyst [9]. The maximum loading per procedure is limited by the solubility of the precursor in the solution. The concentration profile of the impregnated compound depends on the mass transfer conditions within the pores during impregnation and drying. It can be called wet impregnation (WI) or incipient wetness impregnation (IWI), also called dry impregnation, depending on the volume of the impregnating solution being greater than or equal to the pore volume of the support. When pH is not controlled, the pH of the impregnating solution can vary dramatically and often ends up near the support point of zero charge (PZC), at which point the interactions between the metal precursor and support are weakest [8].

2.2 Strong electrostatic adsorption (SEA)

Strong electrostatic adsorption (SEA) is a special case of wet impregnation by which the pH of the precursor solution is set to the pH that yields the strongest electrostatic interactions between the metal ions in solutions and the support [8].

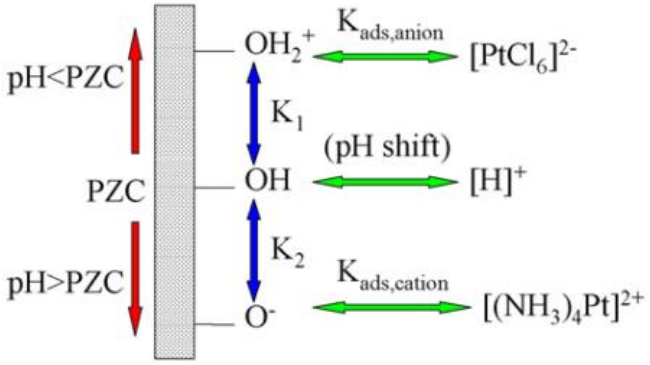

Figure 1 Mechanism of electrostatic adsorption [8]

Brunelle described that the adsorption of precious metal complexes on oxide supports always has electrostatic interactions between electrically charged particles in nature. The hydroxyl groups that inhabit oxide surfaces in contact with aqueous solutions become protonated and therefore positively charged when solution pH is below the point of zero charge (PZC) of the oxide. This positively charged surface adsorbs anions such as hexachloroplatinate(IV) $[PtCl_6]^{2-}$. Conversely, the surfaces become deprotonated or negatively charged when solution pH is above their PZC. The oxide surfaces will then adsorb cations like tetraammineplatinum(II) $[(NH_3)_4Pt]^{2+}$. The hydroxyl groups are neutral when solution pH equals to the PZC of the oxide. This surface adsorption is illustrated in Figure 1 [8].

2.3 Non-Faradaic Electrochemical Modification of Catalytic Activity (NEMCA)

The Non-Faradaic Electrochemical Modification of Catalytic Activity (NEMCA) is a process by which, when electrical potential differences are imposed on two catalyst electrodes separated by an electrolyte, the catalytic rate of the formation of a product at one or more of the catalysts is enhanced above that which could possibly be attained were the reaction purely electrochemical. The effect which appears to defy Faraday's laws of electrolysis can be justified by firstly considering an electrochemical

cell with two electrodes made of Au and Pt which are respectively the cathode and the anode and exposed to the same bulk of a gas mixture consisting of CH_4, O_2, and an inert gas. The generation of CO_2 from the conventional combustion reaction and its electrochemical analogue at the anode are respectively:

$$CH_4 + 2O_2 \longrightarrow CO_2 + 2H_2O \qquad E1$$

$$CH_4 + 4O^{2-} \longrightarrow CO_2 + 2H_2O + 8e^- \qquad E2$$

O^{2-} in reaction E2 is the charge carrier in solid oxide electrolytes frequently employed for high temperature electrochemical reactions and hence its net consumption is proportional to the electrical current observed during electrolysis. By stoichiometry, the formation of CO_2 by reaction E2 must also be linearly dependent on the current generated by this reaction and thus can be at most as high as the equivalent rate governed by the observed current. If only reaction E2 is active, an increase in the current always results in a predictable and linear increase in the rate of CO_2 formation. However, with both E1 and E2 simultaneously active, an increase in the current may lead to a tremendous and non-linear increase in the rate of CO_2 formation which exceeds that possibly achieved solely electrochemically. The excess increase in the rate is attributed to the enhancement of the conventional combustion reaction E1.

The enhancement of the conventional combustion reaction is explained in terms of formation of a promoter species, i.e. O atoms strongly adsorbed on the catalyst working electrode. This species originates from O^{2-} migration in the solid electrolyte due to the applied electromotive force showed in figure 2 to the anode-electrolyte-gas three-phase boundaries.

There, O^{2-} is oxidized to O and then back-spills to the metal surface, thereby forming an effective electronic double layer as shown in Figure 3 and increasing the work function of the catalyst anode. This favors the dissociative adsorption of electron donor molecules, which are generally hydrocarbons for combustion reactions and hence CH_4 in this example, but disfavors the dissociative adsorption of electron acceptor molecules, which are O_2 in this case. These induced changes in the adsorption characteristics can actually lead to both acceleration and inhibition of the catalytic rate of a reaction but for methane combustion they result in rate enhancement

because the adsorption coverage of alkane at catalyst surfaces is known to be relatively minimal compared to that of oxygen. Depending on reactions, the rates can be increased, depending on reactions, 100 to 1 000-fold of the base rates at open circuit conditions.

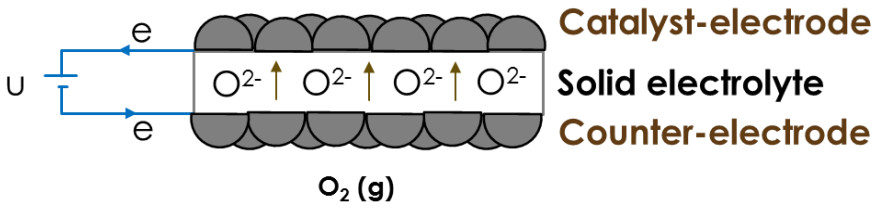

Figure 2 Migration of O^{2-} through solid oxide electrolyte due to an applied potential difference [4]

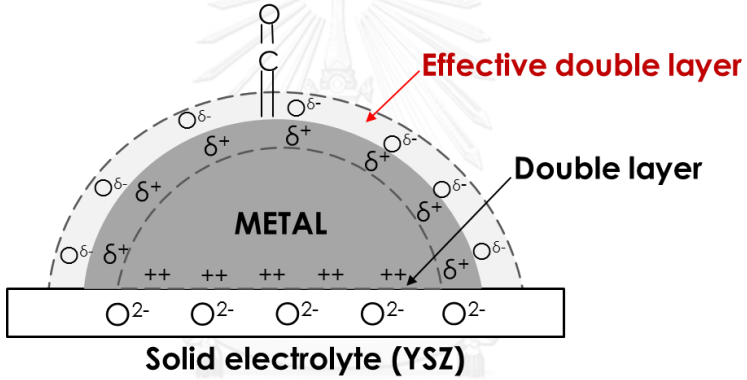

Figure 3 Back spillover of O^{2-} to the anode surface forming an effective electronic double layer [4]

The migration of O^{2-} necessary for NEMCA effects is generated by the 'oxygen pumping' reaction:

$$O_2 + 4e^- \leftrightarrow 2O^{2-} \qquad E3$$

The reaction proceeds to the right side of the equation at the three-phase boundaries of the cathode and to the left side at those of the anode, thus forcing a net movement of O^{2-} from the cathode to the anode. Ideally, the ions are desired to stay at the catalyst surfaces and not to be spent. In reality, they are consumed in both reaction E2 and E3, so the ions must be constantly supplied and this leads to a minimal electrical energy requirement in this kind of systems.

2.4 Platinum

Platinum is a silver-gray lustrous malleable ductile metal. Its crystal structure at ambient conditions is face-centered cubic. Compounds of this element are generally found with oxidation states +2 and +4, and less commonly +1, +5, and +6. Some chemical properties are tabulated in table 1. Platinum is unaffected by air at any temperature. It reacts with boiling aqua regia with the formation of chloroplatinic acid and with molten alkali cyanides. Halogens, cyanides, sulfur, molten sulfur compounds, and hydroxides can affect platinum [10].

Table 1 The chemical property of platinum [10]

Property	Value
Atomic mass	195.078
Atomic number	78
Density (calculated)	21.447 g/cm^3
Melting point	1773.5 ± 1 ℃
Boiling point	approximately 3827 ℃

Platinum can be found in sulfide and arsenide minerals as sperrylite $PtAs_2$, cooperite (Pt,Pd)S, and braggite (Pt,Pd,Ni)S. It is used in many areas such as the automotive, electronic, chemical, jewelry, dental, and glass industries. Platinum is widely used as a catalyst in hydrogenation, dehydrogenation, and isomerization reactions, possessing versatile catalytic qualities. In particular, it is also one of the catalysts in catalytic converters in car exhaust systems. Platinum usage in automotive industries alone composes 80% of the global consumption. The platinum emission rate has been estimated at 0.5-0.8 μg Pt/km from traffic. [10].

2.5 Yttria-stabilized zirconia (YSZ)

Yttria-stabilized zirconia (YSZ) is a ceramic which has a structure of zirconium dioxide (ZrO_2) and stabilized at room temperature by addition of yttrium oxide (Y_2O_3)

as depicted in figure 4. The addition of yttria to pure zirconia replaces some of the Zr^{4+} ions in the zirconia lattice with Y^{3+} ions. This produces oxygen vacancies because three O^{2-} ions replace four O^{2-} ions [11]. It also allows YSZ to conduct O^{2-} ions and therefore conduct an electrical current, provided there is sufficient vacancy site mobility, a property that increases with temperature. This ability to conduct O^{2-} ions makes yttria-stabilized zirconia well suited to be used in solid oxide fuel cells, although it requires high operating temperatures.

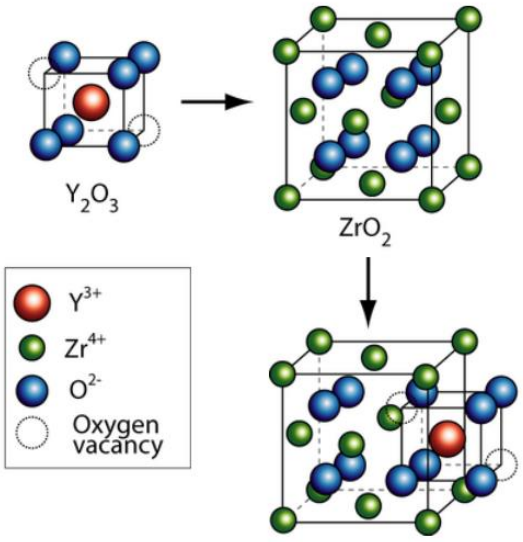

Figure 4 YSZ cubic fluorite structure [12]

Pure zirconium dioxide is stable at the room temperature in a monoclinic structure but undergoes phase transformation from monoclinic to tetragonal at around 1 000 ℃ and then to cubic at about 2 370 ℃ [13].

YSZ has a number of applications to illustrate. It is used in the production of a solid oxide fuel cell (SOFC) as the solid electrolyte which enables oxygen ion conduction while blocking electronic conduction. An SOFC with YSZ electrolyte must be operated at high temperature (600 ℃ - 1000 ℃), while YSZ can still retain its mechanical robustness at this temperatures[14]. Moreover, it is used as an electroceramic due to its ion-conducting properties for various applications such as determining oxygen content in exhaust gases and measuring pH in high-temperature steam. Furthermore, its hardness makes it suitable for jewelry and non-metallic knife blades.

CHAPTER III
LITERATURE REVIEWS

3.1 Catalyst synthesis

There are several methods to prepare metal-supported catalyst, e.g. impregnation, sol-gel, sputtering, and pulsed laser deposition (PLD). The differences in preparations and precursors lead to different of results. Some methods to prepare Pt catalyst deposited on YSZ are presented in table 2.

Last but not least, Jiao and Regalbuto studied the SEA method with many metal ammine complexes: $[Pd(NH_3)_4]^{2+}$, $[Cu(NH_3)_4]^{+2}$, $[Co(NH_3)_6]^{+3}$, $[Ru(NH_3)_6]^{+2}$, $[Ru(NH_3)_6]^{+3}$, and $[Ni(NH_3)_6]^{+2}$ over amorphous and mesoporous silica and found that the supported catalysts prepared by the SEA method had higher dispersion compared to the catalysts synthesized via dry impregnation (DI) at the same metal loadings [8, 15].

Table 2 Comparison of the Pt catalyst deposited on YSZ reported in different references.

Preparation method	Precursors	Average diameter	Characterization method	Ref.
Thin coating	YSZ disc, Pt	unreported	SEM	[16]
Sputtering	YSZ pellet, Pt	unreported	-	[7]
Impregnation	H_2PtCl_6, YSZ powder	~50nm. (Pt)	TEM	[17]
Pulsed laser deposition (PLD)	Pt (1 1 1), YSZ (1 1 1)	20-50 nm.	HRSEM	[18]
Sol–gel method	Zirconium tetra-n-butoxide, $Y(NO_3)_3$,Pt salt	<50nm. (Pt), <50nm. (YSZ)	FE-SEM	[19]
Sol–gel method	$PtCl_4$, $Y(NO_3)_3$,$ZrOCl_2$	~100nm.(Pt), ~100nm.(YSZ)	SEM	[20]

3.2 Electrochemical promotion

The phenomenon was observed unexpectedly by Vayenas and his then student, Stoukides [21] and has been studied in a large number of catalytic systems since. Most prominent reactions observed with NEMCA effects include CO oxidation [22-25], CO_2 hydrogenation [26, 27], methane oxidation [28-33], ethylene oxidation [34-39], NO_x reduction [40-43], propylene oxidation [22, 34, 44, 45], and propane oxidation[1-3, 5-7, 16, 46-51]. The pioneer team has developed a simple mathematical model explaining the phenomenon based on the concept described earlier in section 2.2 [4, 52], although Metcalfe proposed an alternative explanation derived with the absolute rate theory [53, 54].

The phenomenon is categorized into four types (Figure 5): pure electrophobia, pure electrophilia, volcano, and inverted-volcano, according to changes in reaction rates with respect to changes in electrode potential. Most reactions are apparently able to exhibit more than one type of the four behaviors depending on reaction conditions and catalysts. Propane oxidation at Pt, for example, exhibits purely electrophobic behaviour at low propane partial pressure [47] but inverted-volcano behavior at high propane partial pressure [55].

The inverted-volcano behavior is particularly interesting as the rates of reactions falling into this category can be enhanced by both positive and negative electrode potential. One could envisage an electrochemical pellet cell capable of improving reaction rates by both of its catalyst electrodes. A reacting gas mixture could be passed over both electrodes without any partition, which would be required to prevent the mixture from contacting the inhibiting electrode were the NEMCA behavior purely electrophilic or purely electrophobic. However, the inverted-volcano behavior as well as the critical condition for the transition from other behaviors to this are not well understood. Brosda and Vayenas [52] hypothesized that the inverted-volcano type is triggered by weak adsorption of both the electron donor and acceptor, but Pliangos et al. [39] had demonstrated that, for ethylene oxidation, the transition from pure electrophobia to inverted-volcano was achieved by increasing the partial pressure of ethylene from 0.4 to 5.6 kPa while keeping the oxygen partial pressure constant at

1.45 kPa for both cases (Figure 6). Similar transition for propane oxidation was also initiated by increasing the partial pressure of the electron donor as already mentioned in the previous paragraph. Kokkofitis et al. [55] pointed out that decreasing the ratio of the partial pressure of the electron acceptor to that of the electron donor (pA/pD) may cause the transition from pure electrophobia to inverted-volcano, but the latter is observed at pA/pD of 10 in his same paper while Vernoux et al. [47] showed the electrophobic behavior at pA/pD of only 5. The main difference of the two works was that the partial pressure of propane set by Kokkofitis et al. was 1 kPa, while that set by Vernoux et al. was only 0.2 kPa. Therefore, it is better to hypothesise that increasing the partial pressure of the electron donor, rather than decreasing pA/pD, results in the transition from purely electrophobic behavior to inverted-volcano behavior

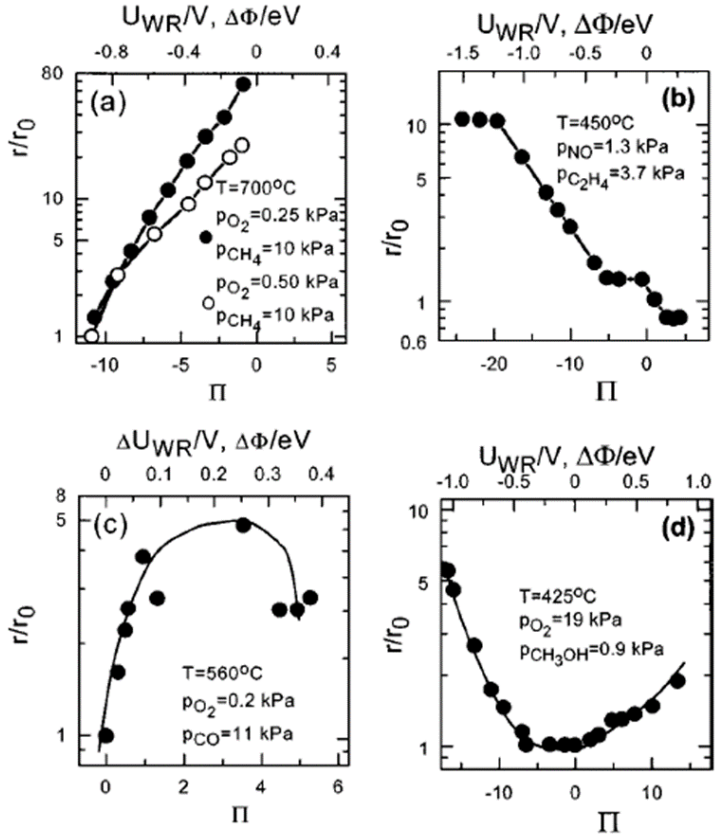

Figure 5 Examples of the four types of NEMCA behaviors [4]. r/r_0 represents the ratio of the rate when a potential difference ΔU_{WR} between the working electrode and the reference electrode is imposed to the rate at the open circuit condition.

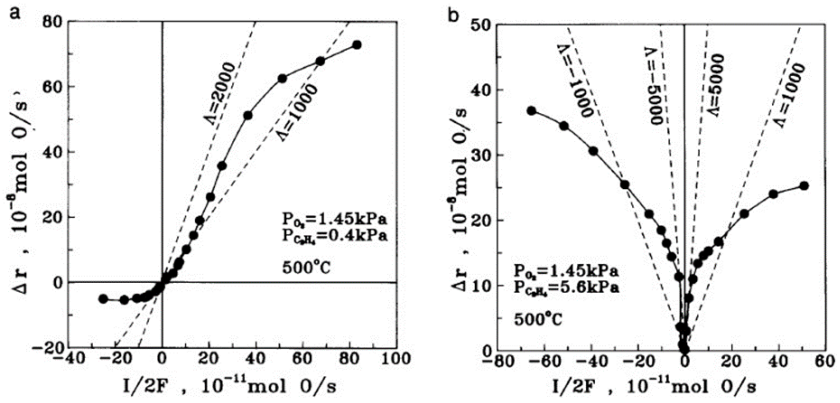

Figure 6 Transition from purely electrophobic behavior to inverted-volcano behavior of ethylene oxidation by increasing the partial pressure of ethylene while keeping the oxygen partial pressure constant [39].

The conventional fabrication of electrodes for NEMCA studies is application of fine metal particle pastes on ionic conductors followed by calcination, although sputtering of metal catalysts on ionic conductors has been practiced recently. These methods provide porous electrode layers with good electrical conductivities but lead to significant portions of catalysts being inactive and serving only as electrical connectors. There are only a relatively small number of papers describing the fabrication and performance of highly dispersed catalysts as electrodes with NEMCA effects. Pt, Pd, or Rh were dispersed on SiO_2, γ-Al_2O_3, ZrO_2, or TiO_2 powders as electrodes on YSZ pellets for the oxidation of CO, C_2H_4, and NO reduction by CO [56]. Enhanced catalytic activity was found to depend not only on the metal catalysts but also the supports. A similar study focusing on the oxidation of C_2H_4 was also published by the same group [57]. Pt dispersed on a porous Au layer deposited on YSZ ionic conductors for the oxidation of C_2H_4 was reported [58]. Carbon-supported Pt electrodes on polybenzimidazole (PBI) were fabricated for methane oxidation, NO reduction, and Fischer-Tropsch synthesis at a relatively low temperature range of 130-175 °C [59]. Pt black on carbon cloth electrodes with Nafion 117 as an ionic conductor were made for CO oxidation at 30 °C [60] and for the water-gas shift reaction at the same temperature [60]. Pt/C electrodes on K-β"Al_2O_3 disc were used for CO and C_3H_6 oxidation [51]. Ni- or Ru-impregnated carbon nanofibre electrodes deposited on YSZ were fabricated for CO_2 hydrogenation [61]. Pt nanoparticles dispersed in the pores of

LSCF-GDC were employed for propane oxidation[62]. Pd was impregnated on highly porous YSZ supports for methane combustion [33].

Table 3 Comparison of faradaic efficiency and rate enhancement ratio of propane oxidation reported in different references

Preparation method	Catalyst	Temperature	Result	References
Sputtering	Pt-YSZ	400 °C	Λ = 1×10^6	(Billard and Vernoux 2005)
Sputtering	Pt-YSZ	350 °C	Λ = 330 ρ = 5.6	(Souentie, Lizarraga et al. 2010)
Pt Paste	Pt-YSZ	420 -520 °C	Λ = 2330 ρ = 1350	(Bebelis and Kotsionopoulos 2006)
Pt Paste	Pt-YSZ	350–500 °C	ρ = 1400	(Kokkofitis, Karagiannakis et al. 2005)
Sputter-deposited Pd film on YSZ	Pd-YSZ	320–450 °C	Λ= 250 ρ = 3	(Peng-ont, Praserthdam et al. 2012)

Wiring between the working electrode and the counter-electrode of a cell is another complication of NEMCA systems. A few works aimed to relieve this constraint by introducing alternative cell layouts. NEMCA was achieved with an isolated Pt electrode positioned between two Au electrodes between which potential differences were imposed (Figure 7) [58]. Effects of the shapes of isolated Pt electrodes were studied [63]. An alternative design of Rh bipolar electrodes exhibited electrochemical promotion for NO reduction (Figure 8) [64]. It was also possible to remove wiring completely by using a mixed protonic-electronic conductor and imposing

electrochemical potential differences through different gas compositions on the two sides of a cell [65, 66].

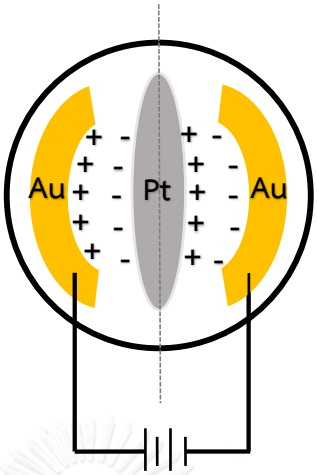

Figure 7 Wireless NEMCA reactor configuration by Marwood et al. [58].

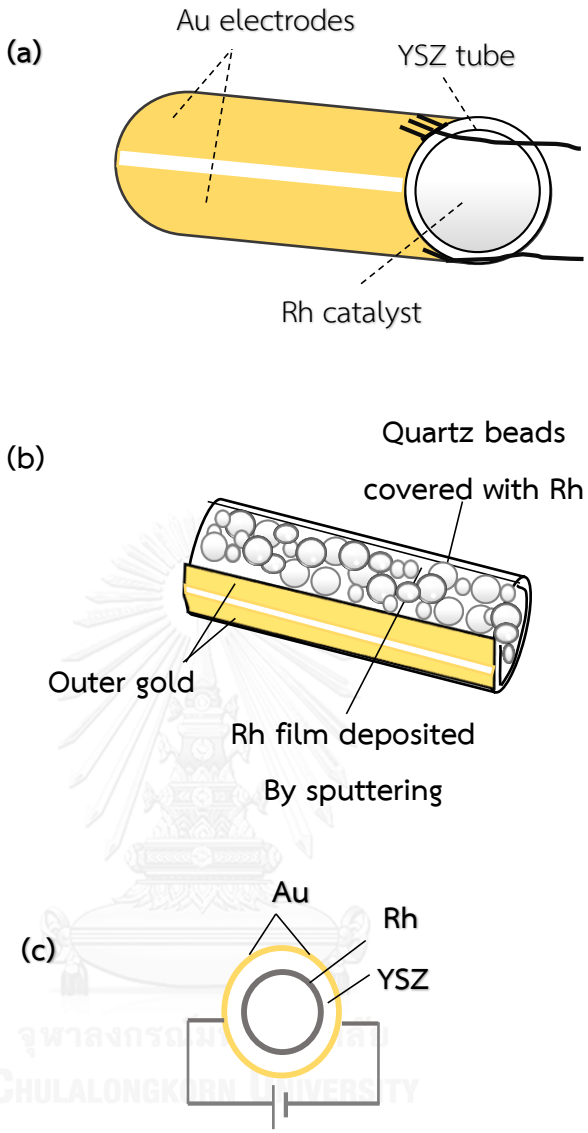

Figure 8 Bipolar NEMCA reactor designed by Pliangos et al. [64]: (a) tube reactor without packing materials, (b) tube reactor with Rh-coated quartz beads, and (c) schematic cross section of the tube reactor.

CHAPTET IV
METHODOLOGY

This chapter divided in four sections, to begin with determination of optimum conditions for SEA. Next, Pt-YSZ cell prepared by SEA with the optimal condition in the first step and Pt-YSZ cell prepared by WI which has surface loading of Pt equal to SEA. After that, do NEMCA experimental. Finally, catalyst was characterized by CO chemisorption technique.

4.1 Determination of optimum conditions for SEA

Optimum conditions for the deposition of Pt on YSZ were determined prior to the actual preparation of the supported catalyst. The point of zero charge (PZC), at which the metal ion-support interactions are at a minimum, were determined by surface loading experiments [8]. A calculated amount of 8 mol% Y_2O_3 stabilized ZrO_2 nano powder (Inframat Advanced Material) was added to aqueous solutions of different initial pH prepared by HNO_3 and NaOH to achieve a 50 mL suspension with a surface loading of 1 000 m^2 L^{-1}. The suspensions were shaken for 1 h, which has been shown to be sufficient for equilibration [67]. Subsequently, the final pH were measured and plotted against the initial pH to identify the plateau of PZC.

The strongest adsorption of Pt on YSZ from aqueous solutions of chloroplatinic acid, $H_2PtCl_6 \cdot 6H_2O$ (Aldrich) occurs at a pH below the PZC of YSZ, at which the surfaces of YSZ are positively charged and thus attract the Pt anion. The optimum pH was determined by adsorption experiments. 200 ppm of chloroplatinic acid in suspensions of 1 000 m^2 L^{-1} YSZ at different initial pH were left to equilibrate for 1 h. The differences in the concentrations of Pt between the initial state and the final state determined by ICP-AES were converted to amounts of Pt adsorbed on YSZ. The surface metal densities of Pt adsorbed on YSZ, calculated by dividing the changes in the concentrations of the metal precursor divided by the surface loading (SL) at 1 000 m^2 L^{-1}

$$\Gamma_{Metal} = (C_{metal,initial} - C_{metal,final})/SL \qquad E4$$

The strongest adsorption of Pt on YSZ is also a function of the concentrations of the Pt precursor. The experiments for the determination of the optimum initial Pt concentration were conducted similarly to the previous experiments with different initial concentrations of Pt precursors instead and at the same initial pH of 3. YSZ-free control experiments were also conducted in parallel.

4.2 Pt-YSZ cell preparation

Au was sputtered on two equal opposite segments on the same side of a YSZ disk of 20 mm diameter and 1.2 mm thickness. A 10 mm-width stripe of bare YSZ was left in the middle for later Pt deposition (Figure 9).

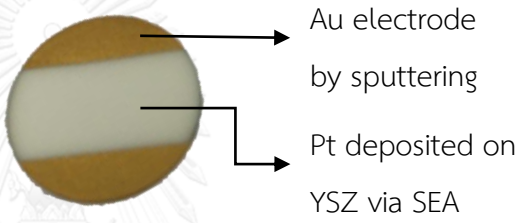

Figure 9 Pt-YSZ cell used in NEMCA experiments

4.2.1 Cell preparation by SEA

After the Au segments were masked, the deposition of Pt was conducted by submerging the cell in 50 ml of 63.5 ppm chloroplatinic acid aqueous solutions at pH ca 3 for 1 h. Subsequently, the masks were removed. The cell was dried overnight in flowing air and was reduced at 250 °C with pure H_2 (30 ml./min) gas for 2 h [68].

4.2.2 Cell preparation by WI

After the Au segments were masked, the deposition of Pt was conducted by dropping 100 µl of chloroplatinic acid aqueous solution that make the surface loading of Pt equal to cell preparation by SEA, the calculation of quantity of chloroplatinic acid solution illustrated in appendix A. Subsequently, the masks were removed. The cell was dried overnight in flowing air and was reduced at 250 °C with pure H_2 (30 ml./min) gas for 2 h.

4.3 NEMCA experiments

Two Au wires were attached to the two Au electrodes at the YSZ disk at one ends and the others were connected to a potentiostat or a power supply so that a potential difference of 6-30 V could be imposed on the two Au electrodes. The Pt-YSZ cell was placed inside a quartz vessel inside a furnace.

Propane was chosen as model light hydrocarbon residuals in exhaust and its oxidation was chosen as a model reaction. The reaction was carried out with 0.27 kPa of C_3H_8 and 1.35 kPa of O_2 for complete combustion at 200-480 °C. The flow rates of the reactants, which consist of 3% propane in helium, Linde, 10% oxygen in helium, Linde and ultra-high purity helium (99.999%), Linde, were set appropriately to achieve the desired partial pressures. At various temperatures and potential differences, the gas product stream was analyzed with an online IR spectrometry for CO_2 concentrations, which could be converted into faradaic yields and rate enhancement ratios by using equation E5 and E6, respectively. The diagram of the experimental apparatuses is shown in Figure 10.

$$\Lambda = (r-r^{\circ})/(I/nF) \qquad \text{E5}$$

$$\rho = r/r^{\circ} \qquad \text{E6}$$

where r° is the catalytic rate at open circuit, r is the electrochemically promoted catalytic rate, I is the applied current, n is the charge of the promotion ion, and F is Faraday's constant (96 485 C mol^{-1}) [4].

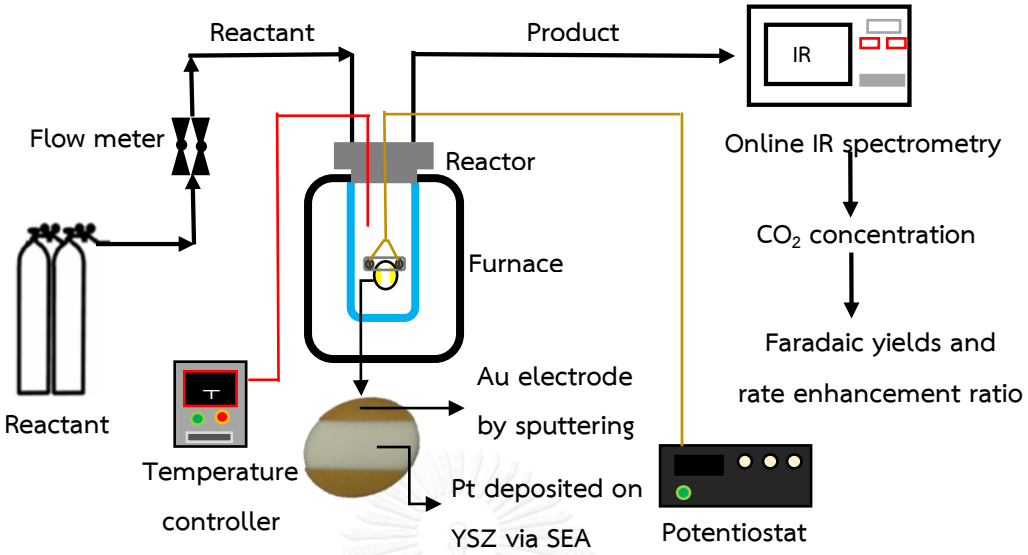

Figure 10 Schematic diagram of the experimental apparatuses

4.4 Procedures of NEMCA for propane oxidation

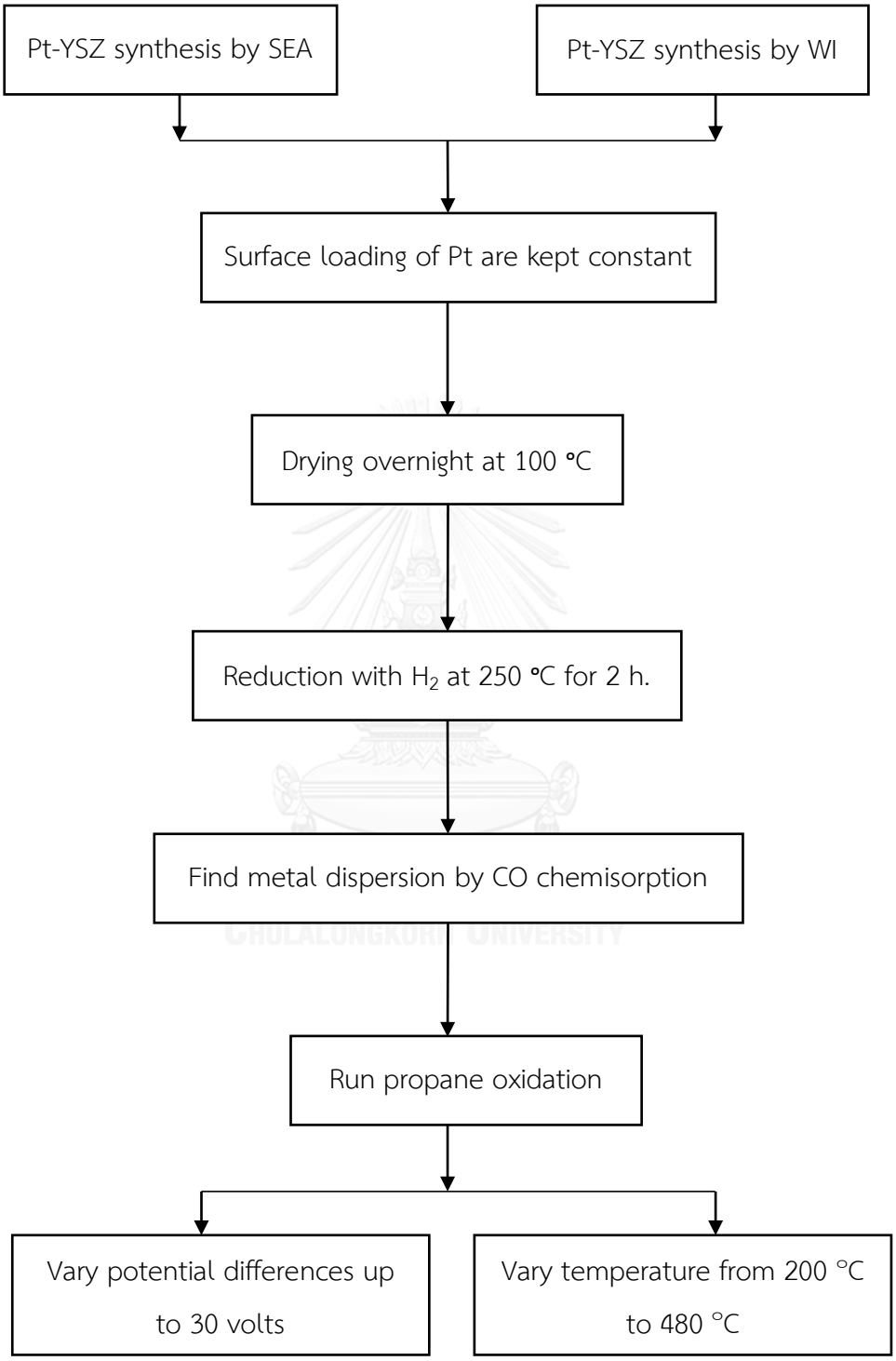

Figure 11 Procedures of NEMCA for propane oxidation

4.5 Carbon monoxide chemisorption

CO chemisorption was carried out following the procedure using a micrometrics chemisorb 2750 Pulse Chemisorption System with ChemiSorb TPx software for measuring the amounts CO chemisorbed on catalyst.

The quartz wool was put into the bottom of quartz tube. Approximately 0.5 g of catalyst was placed in a quartz tube, and then the quartz tube was set up to TPx. Before chemisorption, the catalysts were reduced with 30 ml/min of H_2 at 250 $^{\circ}$C for 2 hours after ramping up at heating rate of 10 $^{\circ}$C /min. Then, 20 microliter of carbon monoxide was inject to catalyst at room temperature and repeated until desorption peak constant. Amount of carbon monoxide adsorption on catalyst was relative to active site. Finally, CO chemisorption can use to determine the metal dispersion percentage.

CHAPTET V
RESULTS AND DISCUSSION

This chapter describes the details about optimum conditions for SEA. The effects of preparation method, potential difference, and temperature on reaction rate. In addition, catalyst characterization by CO chemisorption

5.1 Optimum conditions for SEA

Figure 12 shows the pH shifts of YSZ particles at a surface loading of 1 000 m^2 L^{-1} with and without any Pt precursor in the solutions. The PZC of YSZ was found to be at pH 5 from both curves and is not expected to vary with surface loadings, suggesting that the optimum pH for the adsorption of Pt from $[PtCl_6]^{2-}$ should be below 5. The pH shift curve in the presence of the Pt precursor, denoted by 'Adsorption experiment', displays similar characteristics as those of the metal-free control experiment.

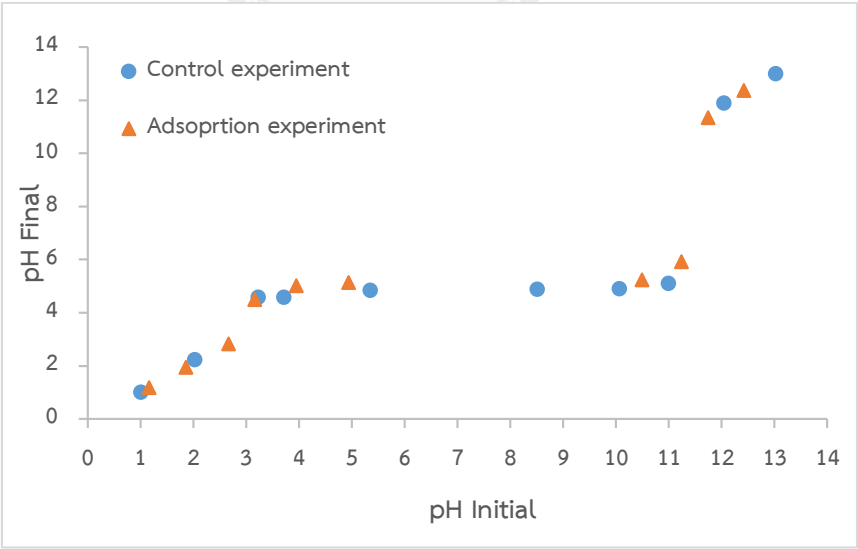

Figure 12 pH shifts of YSZ suspensions at 1 000 m^2 L^{-1} with and without the metal precursor

Figure 13 presents the surface metal densities of Pt adsorbed on YSZ, calculated by dividing the changes in the concentrations of the metal precursor divided by the surface loading (SL) in E4 at 1 000 $m^2 L^{-1}$ in the initial pH range of 1-5, i.e. below the PZC. The maximum adsorption occurred between pH 3-4.5. Figure 14 shows the surface metal densities versus the final Pt concentrations in solutions at 1 000 $m^2 L^{-1}$. The initial concentrations were varied from 50 to 600 ppm. The adsorption curve indicates that the adsorption increases to reach the maximum adsorption at a final concentration of ca 63.5 ppm. The adsorption at higher concentrations is even lower than that at lower concentrations, which is caused by the effect of high ionic strength [8]. Once the YSZ is saturated, the additional chloroplatinic acid remains in solution, increasing the ionic strength.

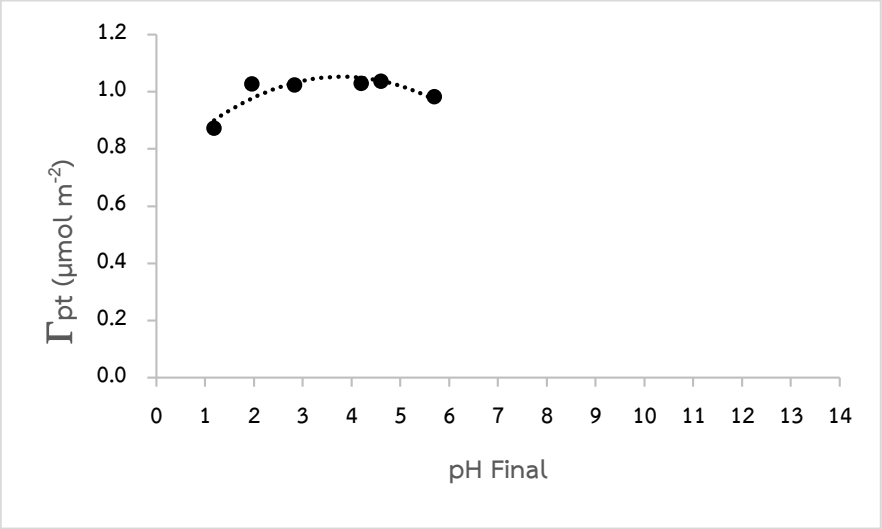

Figure 13 Dependence of surface metal densities on solution final pH (initial Pt precursor concentration of 200 ppm)

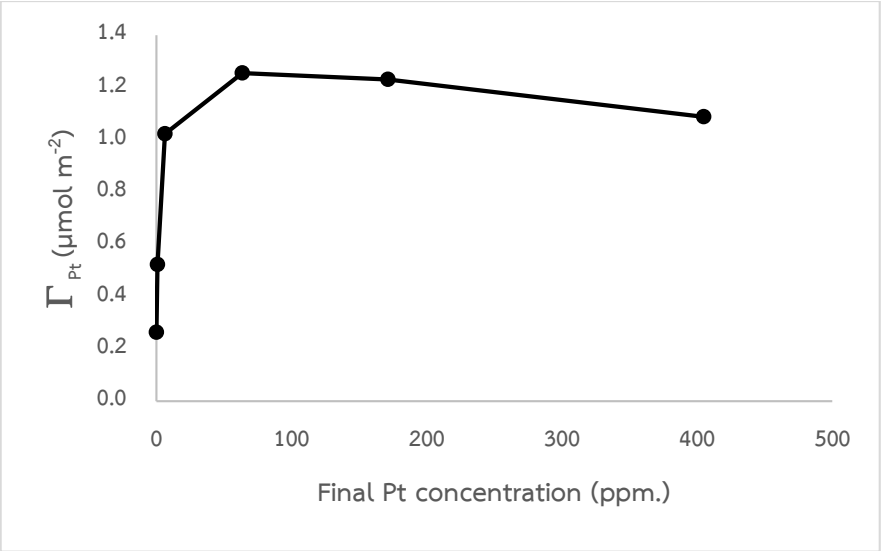

Figure 14 Dependence of surface metal densities on final Pt concentrations at a final pH of 4.5

To sum up, the maximum adsorption occurred between pH 3-4.5 and the surface metal densities of Pt approximate 1.228 μmol m^{-2} which means platinum 239 mg L^{-1} on YSZ 17.071 g L^{-1} Therefore, platinum loading equal to 1.38%. In addition, BET surface area of YSZ powder is 58.5749 m^2 g^{-1}. Then surface loading of platinum equal to 2.396×10^{-8} g Pt cm^{-2}. After that, this surface loading of platinum of both method are kept constant.

5.2 Catalytic activity under open-circuit condition

Propane oxidation reaction was carried out at a Pt-YSZ cell fabricated with the determined optimum conditions. The catalytic CO_2 production rates by SEA method were higher than WI method. Figure 15 shows the catalytic CO_2 production rates by SEA method, which increases from 1.9×10^{-9} mol s^{-1} to 1.7×10^{-8} mol s^{-1} as the temperature increases from 200 to 480 °C. The catalytic CO_2 production rates by WI method which increased from 4.8×10^{-10} mol s^{-1} to 1.3×10^{-9} mol s^{-1} as the temperature increased from 200 to 400 °C. The values then dropped slightly to 4.8×10^{-10} at 480 °C, probably due to catalyst deactivation.

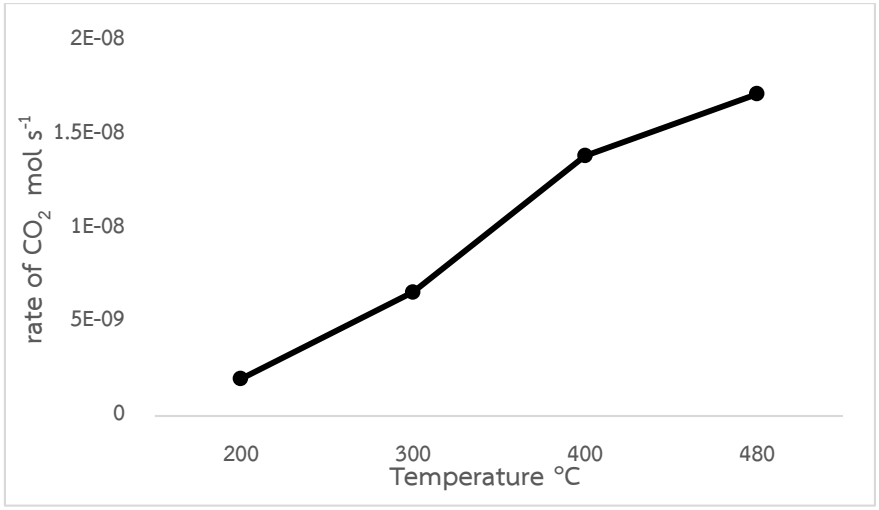

Figure 15 Dependence of open-circuit CO_2 production rates on the temperature by SEA method

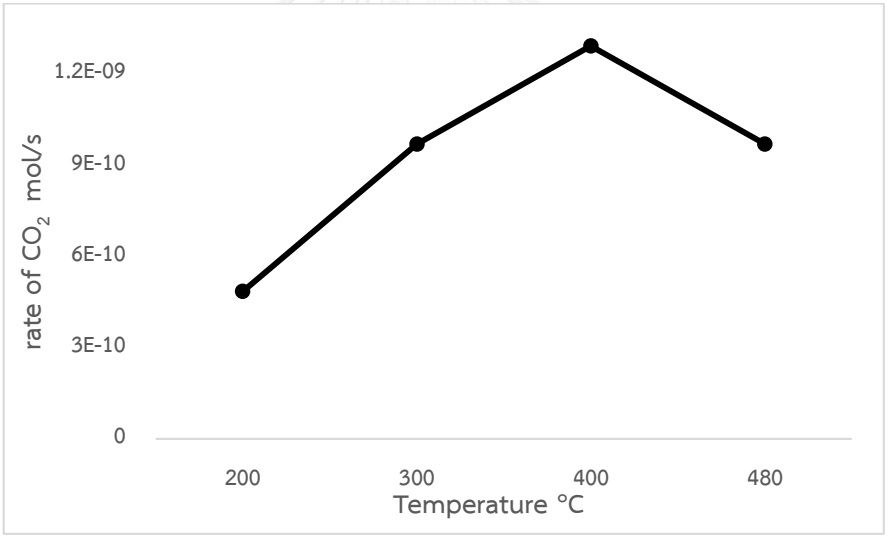

Figure 16 Dependence of open-circuit CO_2 production rates on the temperature by WI method

5.3 Electrochemically promoted catalytic activity with Pt-YSZ by SEA method

The faradaic yields and the rate enhancement ratios at cell voltages up to 30 V at 200 $^{\circ}$C with Pt-YSZ by SEA preparation are showed in Figure 17. The highest faradaic yield of 5.2×10^{4} was obtained at a cell voltage of 6 V and probably second only to the work of Billard and Vernoux in which a value of 1×10^{6} was reported [6],

while common values are generally in the orders of 100-1000. As the cell voltage was increased, the faradaic yield slightly decreased to 1.4×10^4 at 30 V. While the rate enhancement ratios gradually rose from 1.0 to 3.7 as the cell voltage was increased.

As the temperature was increased to 300 °C, the faradaic yields become negative for any cell voltages. Nevertheless, the absolute faradaic yields are still greater than one, suggesting that the reaction exhibits NEMCA. The rate enhancement ratios were below one (Figure 18), indicating that the catalytic rates were suppressed by applied electrical potentials. An explanation for this observation is unavailable at the moment due to the lack of understanding of this relatively new phenomenon.

Figure 19, at temperature 400 °C, it can be seen that the faradaic yields had a rising trend as the cell voltage was increased but the values were still negative. Meanwhile, the rate enhancement ratios were constant at around 0.95 for any cell voltage

Figure 20 provided the faradaic yields when the temperature was increased to 480 °C. The maximum faradaic yield considerably declined to a small value of 1.038 when compared to the faradaic yields at 200 °C (5.2×10^4). The rate enhancement ratios at 480 °C were also smaller than those at 200 °C.

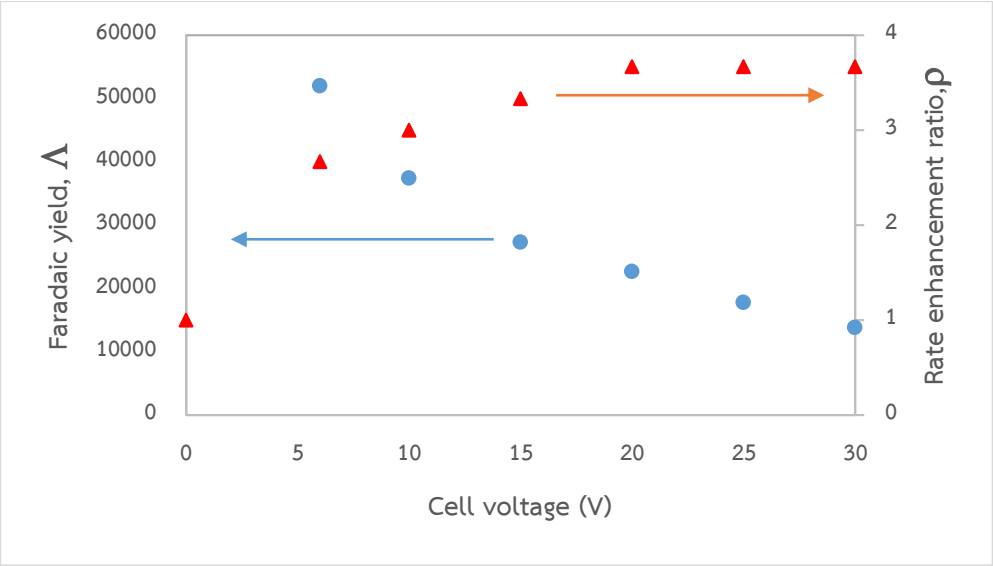

Figure 17 Dependence of faradaic yields and rate enhancement ratio on applied voltages at 200 °C with Pt-YSZ by SEA method

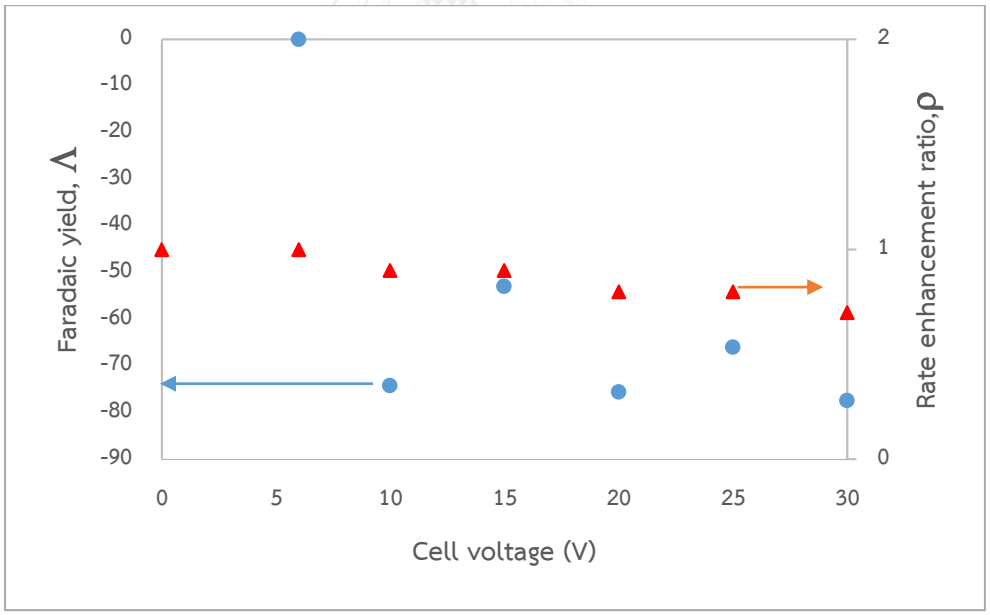

Figure 18 Dependence of faradaic yields and rate enhancement ratio on applied voltages at 300 °C with Pt-YSZ by SEA method

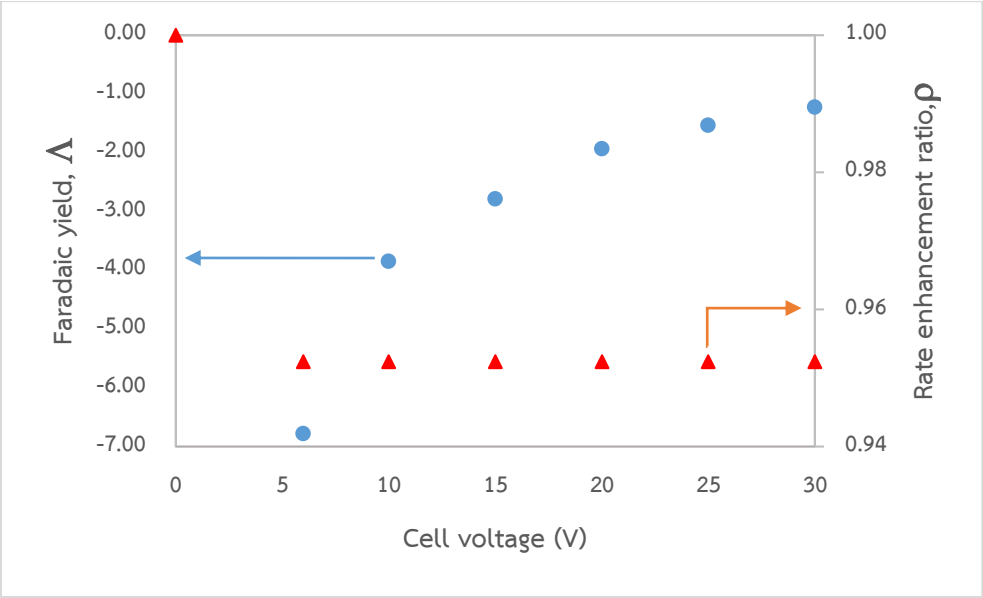

Figure 19 Dependence of faradaic yields and rate enhancement ratio on applied voltages at 400 °C with Pt-YSZ by SEA method

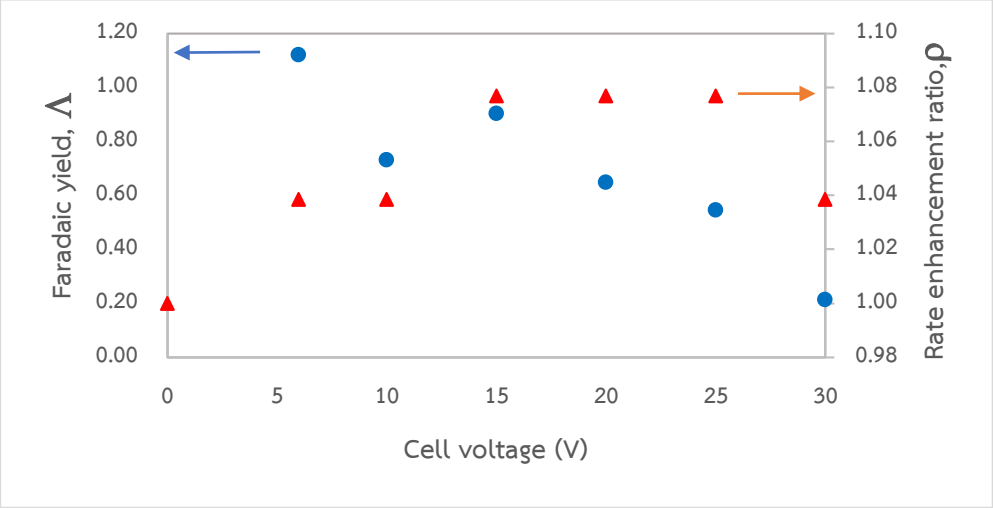

Figure 20 Dependence of faradaic yields and rate enhancement ratio on applied voltages at 480 °C with Pt-YSZ by SEA method

5.4 Electrochemically promoted catalytic activity with Pt-YSZ by WI method

The faradaic yields and the rate enhancement ratios at cell voltages up to 30 V at 200 °C with Pt-YSZ prepared by WI are presented in Figure 21. The highest faradaic

yield of 1.03×10^4 was obtained at a cell voltage of 6 V. As the cell voltage was increased, the faradaic yield decreased gradually to 1.7×10^3 at 30 V. While the rate enhancement ratios remained constant at 1.333 for every cell voltage.

As the temperature was increased to 300 °C, the faradaic yields equal to zero at 6-15 V, suggesting that NEMCA did not occur. At cell voltages higher than 15 V, the values became negative. At cell voltages of 6-15 V, the rate enhancement ratios were equal to one but were decreased below one at higher voltages (Figure 22).

At 400 °C, Figure 23 as a whole suggests that the trends of the faradaic yield and the rate enhancement ratio were similar to those at 300 °C. At a higher temperature of 480 °C, Figure 24 shows that even though the applied voltages reached 30 V, the faradaic yields were always equal to zero. It can be seen that the rate enhancement ratios in general remained at approximately one for temperatures from 200 to 480 °C

The wireless cell is polarised anodically on the right and cathodically on the left as shown in Figure 25. Then, O^{2-} in YSZ migrates from left to right. Pt particles act as bipolar electrodes. Some cell voltages enhance catalytic CO_2 production rates by promoting the adsorption of oxidized species $O^{\delta-}$ on a fraction of the areas of Pt particles and forms effective double layer (Figure 25 a). Conversely, the suppression of catalytic CO_2 production rates arises from depletion of $O^{\delta-}$ in some areas of Pt particles, which diminishes the effective double layer (Figure 25 b).

The generally poorer faradaic yields and rate enhancement ratios at higher temperatures were expected and explained in terms of higher rates of O^{2-} desorption [4, 69]. High temperatures probably affect some surface interactions and shift the balance between adsorption and desorption rates of O^{2-}. Desorption of O^{2-} is higher than O_2 supply rate at high temperatures. This results in larger anionic area on Pt

particles with diminished coverage of $O^{\delta-}$ and effective electrical double-layer, ultimately leading to weaker NEMCA effects.

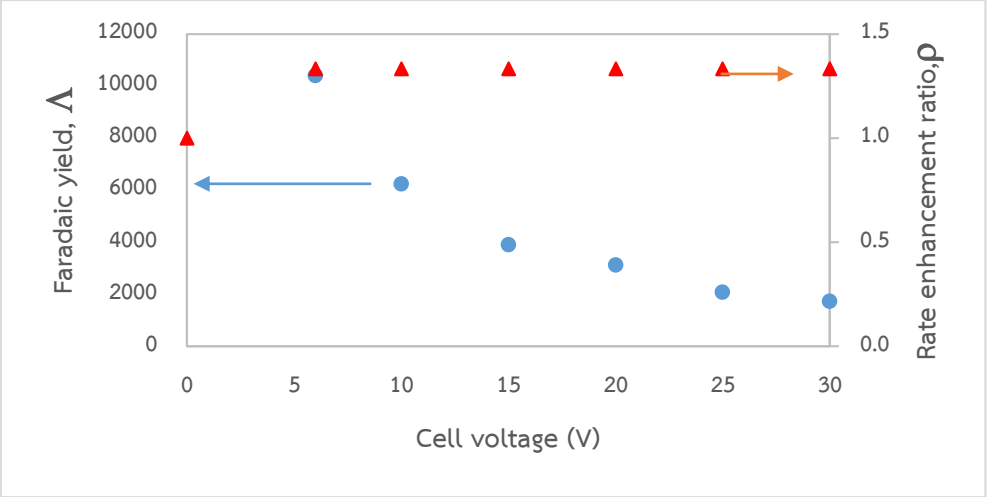

Figure 21 Dependence of faradaic yields and rate enhancement ratio on applied voltages at 200 °C with Pt-YSZ by WI method

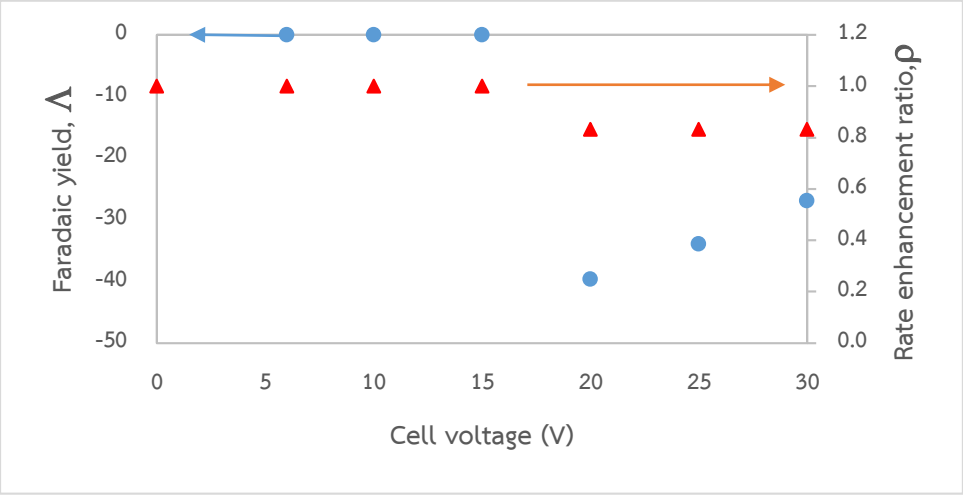

Figure 22 Dependence of faradaic yields and rate enhancement ratio on applied voltages at 300 °C with Pt-YSZ by WI method

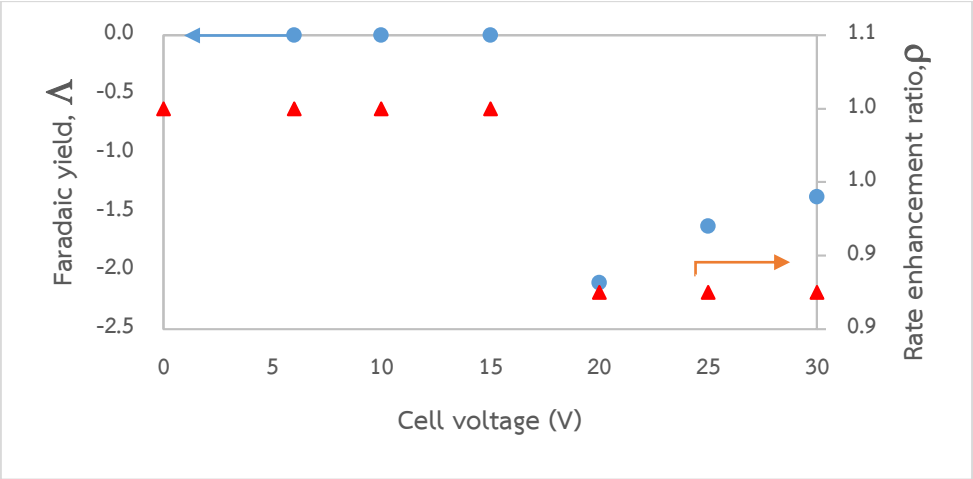

Figure 23 Dependence of faradaic yields and rate enhancement ratio on applied voltages at 400 °C with Pt-YSZ by WI method

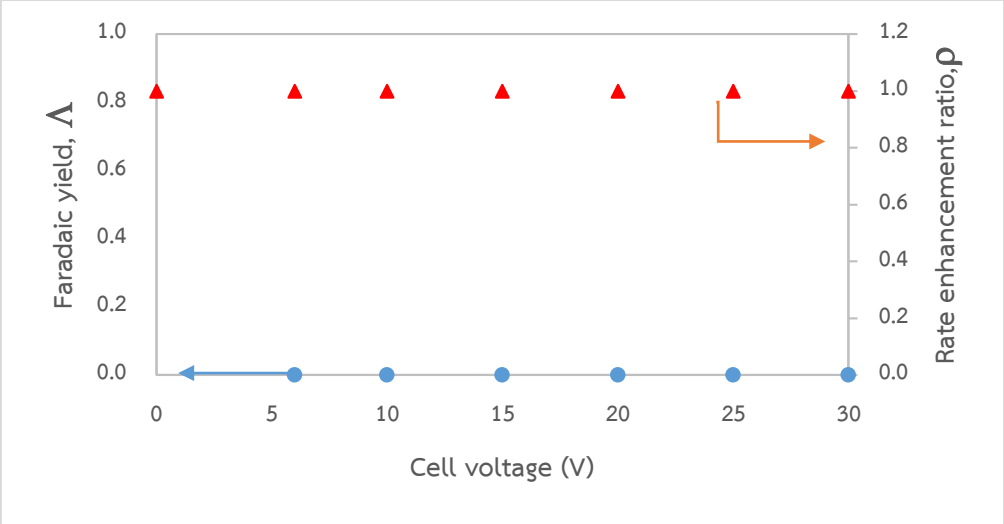

Figure 24 Dependence of faradaic yields and rate enhancement ratio on applied voltages at 480 °C with Pt-YSZ by WI method

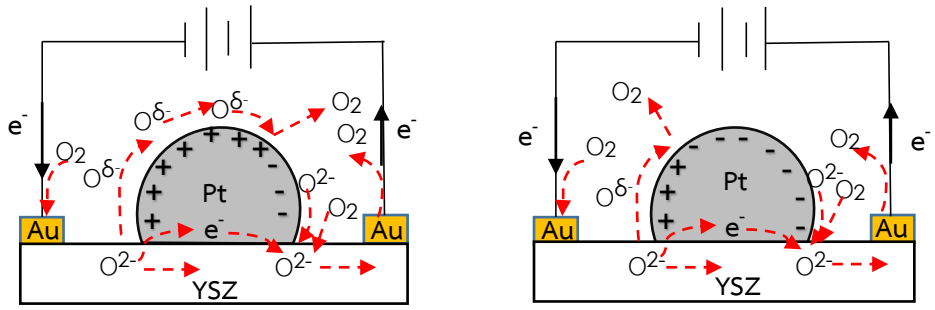

Figure 25 The migration of O^{2-} cover Pt in wireless configuration: favourable condition (a) and unfavourable condition (b)

5.5 Propane conversion with catalyst synthesized via SEA

Generally, it can be seen that the percentages of propane conversion were improved as the temperature increased, being approximate 1.3% at 200 °C to 3.4% at 480 °C. Nonetheless, the values were small despite the applied voltage up to 30 V and temperature increased to 480 °C. At 200 °C, propane conversion rose slightly from 0.36% at open circuit to 1.22% at 15 V and 1.3 % at voltages higher than 15 V. This is the best condition (200 °C) and the conversion increased as the cell voltage increased. In contrast, the value at 300 °C had fallen as the cell voltage increased, which was in agreement with the value of rate enhancement ratio. Whereas at 400 °C, %conversion remained almost constant at 2.4%. Accordingly, the temperature influences the propane conversion more than the applied voltages do (Figure 26). At 200 °C and applied cell voltage of 15 V, the catalytic CO_2 production or %conversion equalled to the open-circuit propane oxidation rate at 300 °C. Hence, the propane oxidation rates at 200 ℃ could be raised to the open-circuit value at 300 ℃ by only the application of electric potential.

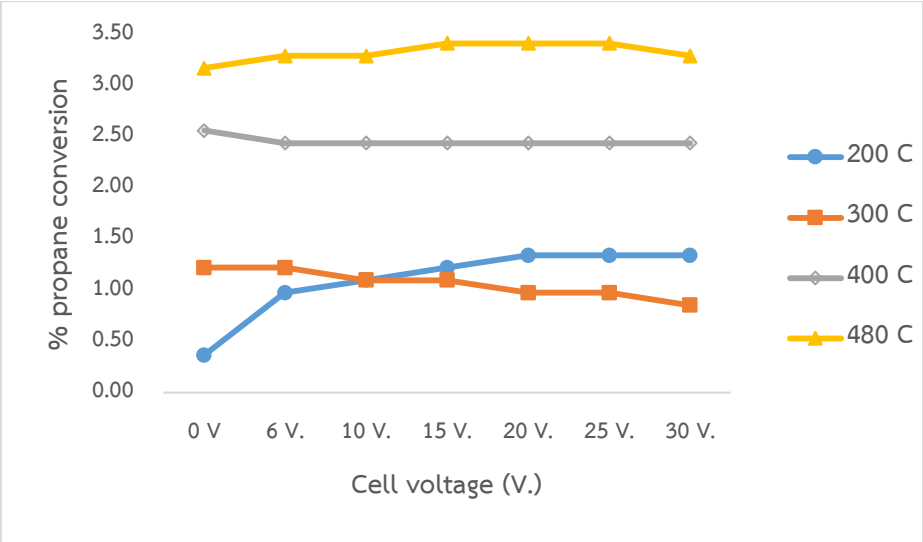

Figure 26 Effect of temperature and cell voltage on propane conversion with catalyst synthesized by SEA

5.6 Propane conversion with catalyst synthesized via WI

In general, the notable point is that the propane conversion was below one. The highest propane conversion was 0.9% at 400 °C at 0-15 V. The least propane conversion was 0.36% at 200 °C and open-circuit condition. At 300-400 °C, when the applied voltage was at 30 V, the percentages of propane conversion did not differ from that at open-circuit condition, but dropped at voltages greater than 15 V. The results were in agreement with the rate enhancement ratios. The catalysts prepared by the SEA method (Figure 25) had higher %conversion compared to the catalysts synthesized via WI (Figure 26). Therefore, the preparation method affected the NEMCA performance.

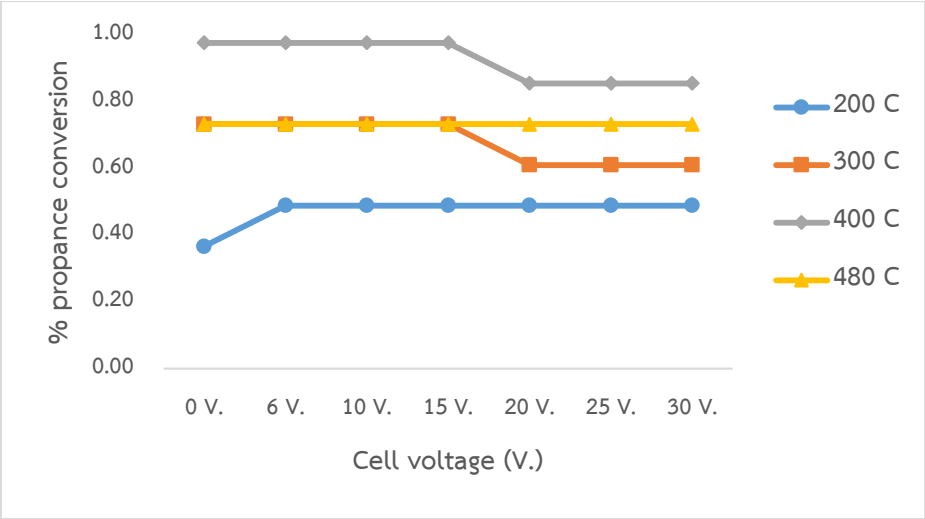

Figure 27 Effect of temperature and cell voltage on propane conversion with catalyst synthesized by WI

5.7 Catalyst characterization

The differences in the faradaic yields, rate enhancement ratios, and propane conversion between the catalysts prepared by SEA and WI were thought to be caused by the differences in the distribution of Pt on YSZ despite the same surface loadings. Determination of the metal dispersion obtained by the two synthesis routes by CO chemisorption shows that the dispersion of platinum deposited on YSZ by SEA of 80.75% was higher than that by WI of 44.35% at the same platinum loading (1.38 %). Likewise, the catalysts prepared by the SEA method had higher dispersion compared to the catalysts synthesized via dry impregnation (DI) was informed by Jiao and Regalbuto [8]. As $O^{\delta-}$ can moves on the surface of Pt particles for some distance before it is desorbed to O_2. Higher metal dispersion means smaller sizes of metal particles, and $O^{\delta-}$ be able to cover the surface of small Pt particle more than large particle. It is hypothesized that the smaller Pt particle sizes prepared by SEA promote high faradaic yields, which are approximately five times the faradaic yields from WI. Furthermore, the rate enhancement ratios seem to very likely depend on the size of the catalyst particles as demonstrated by Marwood et al. [58].

CHAPTET VI
CONCLUSIONS AND SUGGESTION

A large faradaic yield of 5.2×10^4 was achieved at 200 °C and cell voltage 6 V from propane oxidation with Pt deposited on YSZ by SEA method. Moreover, the results is unclear when apply potential voltage at temperature greater than 200 °C. Catalyst prepared by SEA offered higher propane conversion than that prepared by WI. Catalysts prepared by different methods had different metal particle sizes and dispersion. The percentage of metal dispersion via SEA was almost double that by WI. Accordingly, the preparation methods of catalyst affect the efficacy of NEMCA. The catalysts prepared by the SEA works better with NEMCA than that by WI method.

REFERENCES

[1] Kokkofitis, C., Karagiannakis, G., Zisekas, S., and Stoukides, M. Catalytic study and electrochemical promotion of propane oxidation on Pt/YSZ. Journal of Catalysis 234(2) (2005): 476-487.

[2] Kokkofitis, C. and Stoukides, M. Rate and oxygen activity oscillations during propane oxidation on Pt/YSZ. Journal of Catalysis 243(2) (2006): 428-437.

[3] Peng-ont, S., Praserthdam, P., Matei, F., Ciuparu, D., Brosda, S., and Vayenas, C.G. Electrochemical Promotion of Propane and Methane Oxidation on Sputtered Pd Catalyst-Electrodes Deposited on YSZ. Catalysis Letters 142(11) (2012): 1336-1343.

[4] Vayenas, C.G., Brosda, S., and Pliangos, C. Rules and Mathematical Modeling of Electrochemical and Chemical Promotion: 1. Reaction Classification and Promotional Rules. Journal of Catalysis 203(2) (2001): 329-350.

[5] Bebelis, S. and Kotsionopoulos, N. Non-faradaic electrochemical modification of the catalytic activity for propane combustion of Pt/YSZ and Rh/YSZ catalyst-electrodes. Solid State Ionics 177(26–32) (2006): 2205-2209.

[6] Billard, A. and Vernoux, P. Influence of the thickness of sputter-deposited platinum films on the electrochemical promotion of propane combustion. Ionics 11(1-2) (2005): 126-131.

[7] Souentie, S., Lizarraga, L., Papaioannou, E.I., Vayenas, C.G., and Vernoux, P. Permanent electrochemical promotion of C3H8 oxidation over thin sputtered Pt films. Electrochemistry Communications 12(8) (2010): 1133-1135.

[8] Jiao, L. and Regalbuto, J.R. The synthesis of highly dispersed noble and base metals on silica via strong electrostatic adsorption: I. Amorphous silica. Journal of Catalysis 260(2) (2008): 329-341.

[9] Acres, G.J.K., Bird, A.J., Jenkins, J.W., and King, F. The design and preparation of supported catalysts. in Kemball, C. and Dowden, D.A. (eds.),Catalysis: Volume 4, pp. 1-30: The Royal Society of Chemistry, 1981.

[10] Kiilunen, M., Aitio, A., and Santonen, T. Chapter 50 - Platinum∗. in Nordberg, G.F.N.A.F. (ed.)Handbook on the Toxicology of Metals (Fourth Edition), pp. 1125-1141. San Diego: Academic Press, 2015.

[11] H. Yanagida, K.K., M. Miyayama. The Chemistry of Ceramics. John Wiley & Sons, 1996.

[12] Derek Fray, Á.V., Steve Mounsey. Electrolyte Available from: http://www.doitpoms.ac.uk/tlplib/fuel-cells/printall.php

[13] Schlichting, K.W., Padture, N.P., and Klemens, P.G. Thermal conductivity of dense and porous yttria-stabilized zirconia. Journal of Materials Science 36(12) (2001): 3003-3010.

[14] Minh, N.Q. Ceramic Fuel Cells. Journal of the American Ceramic Society 76(3) (1993): 563-588.

[15] Jiao, L. and Regalbuto, J.R. The synthesis of highly dispersed noble and base metals on silica via strong electrostatic adsorption: II. Mesoporous silica SBA-15. Journal of Catalysis 260(2) (2008): 342-350.

[16] Kotsionopoulos, N. and Bebelis, S. Electrochemical promotion of the oxidation of propane on Pt/YSZ and Rh/YSZ catalyst-electrodes. Journal of Applied Electrochemistry 35(12) (2005): 1253-1264.

[17] Bultel, L., Vernoux, P., Gaillard, F., Roux, C., and Siebert, E. Electrochemical and catalytic properties of porous Pt–YSZ composites. Solid State Ionics 176(7–8) (2005): 793-801.

[18] Beck, G., et al. Epitaxial Pt(111) thin film electrodes on YSZ(111) and YSZ(100) — Preparation and characterisation. Solid State Ionics 178(5–6) (2007): 327-337.

[19] Shiga, H., Okubo, T., and Sadakata, M. Preparation of Nanostructured Platinum/Yttria-Stabilized Zirconia Cermet by the Sol−Gel Method. Industrial & Engineering Chemistry Research 35(12) (1996): 4479-4486.

[20] Peng, Z., Liu, M., and Balko, E. A new type of amperometric oxygen sensor based on a mixed-conducting composite membrane. Sensors and Actuators B: Chemical 72(1) (2001): 35-40.

[21] Stoukides, M. and Vayenas, C.G. The effect of electrochemical oxygen pumping on the rate and selectivity of ethylene oxidation on polycrystalline silver. Journal of Catalysis 70(1) (1981): 137-146.

[22] de Lucas-Consuegra, A., Dorado, F., Valverde, J.L., Karoum, R., and Vernoux, P. Electrochemical activation of Pt catalyst by potassium for low temperature CO deep oxidation. Catalysis Communications 9(1) (2008): 17-20.

[23] Xia, C., Falgairette, C., Li, Y., Foti, G., Comninellis, C., and Harbich, W. Electrochemical promotion of CO combustion over Pt/YSZ under high vacuum conditions. Applied Catalysis B: Environmental 113–114(0) (2012): 250-254.

[24] Yentekakis, I.V., Moggridge, G., Vayenas, C.G., and Lambert, R.M. In Situ controlled promotion of catalyst surfaces via NEMCA: The effect of Na on the Pt-catalyzed CO oxidation. Journal of Catalysis 146(1) (1994): 292-305.

[25] Yentekakis, I.V. and Vayenas, C.G. In Situ Controlled Promotion of Pt for CO Oxidation via NEMCA Using CaF2, as the Solid Electrolyte. Journal of Catalysis 149(1) (1994): 238-242.

[26] Papaioannou, E.I., Souentie, S., Hammad, A., and Vayenas, C.G. Electrochemical promotion of the CO2 hydrogenation reaction using thin Rh, Pt and Cu films in a monolithic reactor at atmospheric pressure. Catalysis Today 146(3–4) (2009): 336-344.

[27] Theleritis, D., Souentie, S., Siokou, A., Katsaounis, A., and Vayenas, C.G. Hydrogenation of CO2 over Ru/YSZ Electropromoted Catalysts. ACS Catalysis 2(5) (2012): 770-780.

[28] Frantzis, A.D., Bebelis, S., and Vayenas, C.G. Electrochemical promotion (NEMCA) of CH4 and C2H4 oxidation on Pd/YSZ and investigation of the origin of NEMCA via AC impedance spectroscopy. Solid State Ionics 136–137(0) (2000): 863-872.

[29] Jiménez-Borja, C., et al. Electrochemical promotion of methane oxidation on Pd catalyst-electrodes deposited on Y2O3-stabilized-ZrO2. Applied Catalysis B: Environmental 128(0) (2012): 48-54.

[30] Jiménez-Borja, C., Delgado, B., Dorado, F., and Valverde, J.L. Experimental data and kinetic modeling of the catalytic and electrochemically promoted CH4

oxidation over Pd catalyst-electrodes. Chemical Engineering Journal 225(0) (2013): 315-322.

[31] Nakos, A., Souentie, S., and Katsaounis, A. Electrochemical promotion of methane oxidation on Rh/YSZ. Applied Catalysis B: Environmental 101(1–2) (2010): 31-37.

[32] Roche, V., Karoum, R., Billard, A., Revel, R., and Vernoux, P. Electrochemical promotion of deep oxidation of methane on Pd/YSZ. Journal of Applied Electrochemistry 38(8) (2008): 1111-1119.

[33] Matei, F., et al. Enhanced electropromotion of methane combustion on palladium catalysts deposited on highly porous supports. Applied Catalysis B: Environmental 132–133 (2013): 80-89.

[34] Beatrice, P., Pliangos, C., Worrell, W.L., and Vayenas, C.G. Electrochemical promotion of ethylene and propylene oxidation on Pt deposited on yttria–titania–zirconia. Solid State Ionics 136–137(0) (2000): 833-837.

[35] Kaloyannis, A.C., Pliangos, C.A., Yentekakis, I.V., and Vayenas, C.G. In situ controlled promotion of catalyst surfaces via solid electrolytes: Ethylene oxidation on Rh and propylene oxidation on Pt. Ionics 1(2) (1995): 159-164.

[36] Nicole, J. and Comninellis, C. Electrochemical promotion of oxide catalyst for the gas phase combustion of ethylene. Solid State Ionics 136–137(0) (2000): 687-692.

[37] Nicole, J. and Comninellis, C.H. Electrochemical promotion of IrO2 catalyst activity for the gas phase combustion of ethylene. Journal of Applied Electrochemistry 28(3) (1998): 223-226.

[38] Toghan, A., Rosken, L.M., and Imbihl, R. The electrochemical promotion of ethylene oxidation at a Pt/YSZ catalyst. Chemphyschem 11(7) (2010): 1452-9.

[39] Pliangos, C., Yentekakis, I.V., Ladas, S., and Vayenas, C.G. Non-Faradaic Electrochemical Modification of Catalytic Activity: 9. Ethylene Oxidation on Pt Deposited on TiO2. Journal of Catalysis 159(1) (1996): 189-203.

[40] Béguin, B., et al. Electrochemical promotion of NO reduction by propene on Pt/YSZ. Ionics 8(1-2) (2002): 128-135.

[41] Marwood, M., Kaloyannis, A., and Vayenas, C.G. Electrochemical promotion of the NO reduction by C2H4 on Pt/YSZ and by CO on Pd/YSZ. Ionics 2(3-4) (1996): 302-311.

[42] Vayenas, C.G., Yentekakis, I.V., Bebelis, S.I., and Neophytides, S.G. In Situ Controlled Promotion of Catalyst Surfaces Via Solid Electrolytes: The NEMCA Effect. Berichte der Bunsengesellschaft für physikalische Chemie 99(11) (1995): 1393-1401.

[43] Yentekakis, I.V., Lambert, R.M., Tikhov, M.S., Konsolakis, M., and Kiousis, V. Promotion by Sodium in Emission Control Catalysis: A Kinetic and Spectroscopic Study of the Pd-Catalyzed Reduction of NO by Propene. Journal of Catalysis 176(1) (1998): 82-92.

[44] de Lucas-Consuegra, A., Dorado, F., Valverde, J.L., Karoum, R., and Vernoux, P. Low-temperature propene combustion over Pt/K-βAl2O3 electrochemical catalyst: Characterization, catalytic activity measurements, and investigation of the NEMCA effect. Journal of Catalysis 251(2) (2007): 474-484.

[45] Vernoux, P., Gaillard, F., Lopez, C., and Siebert, E. In-situ electrochemical control of the catalytic activity of platinum for the propene oxidation. Solid State Ionics 175(1–4) (2004): 609-613.

[46] Peng-ont, S., Souentie, S., Assabumrungrat, S., Praserthdam, P., Brosda, S., and Vayenas, C.G. Electrochemical promotion of propane oxidation over Pd, Ir, and Ru catalyst-electrodes deposited on YSZ. Ionics 19(12) (2013): 1705-1714.

[47] Vernoux, P., Gaillard, F., Bultel, L., Siebert, E., and Primet, M. Electrochemical Promotion of Propane and Propene Oxidation on Pt/YSZ. Journal of Catalysis 208(2) (2002): 412-421.

[48] Kotsionopoulos, N. and Bebelis, S. Electrochemical characterization of the Pt/beta"aEuro"Al2O3 system under conditions of in situ electrochemical modification of catalytic activity for propane combustion. Journal of Applied Electrochemistry 40(10) (2010): 1883-1891.

[49] Lizarraga, L., Guth, M., Billard, A., and Vernoux, P. Electrochemical catalysis for propane combustion using nanometric sputtered-deposited Pt films. Catalysis Today 157(1–4) (2010): 61-65.

[50] Roche, V., et al. Electrochemical promotion of propane deep oxidation on doped lanthanum manganites. Ionics 14(3) (2008): 235-241.

[51] de Lucas-Consuegra, A., et al. Preparation and characterization of a low particle size Pt/C catalyst electrode for the simultaneous electrochemical promotion of CO and C3H6 oxidation. Applied Catalysis A: General 365(2) (2009): 274-280.

[52] Brosda, S. and Vayenas, C.G. Rules and Mathematical Modeling of Electrochemical and Classical Promotion: 2. Modeling. Journal of Catalysis 208(1) (2002): 38-53.

[53] Metcalfe, I.S. Electrochemical Promotion of Catalysis: I: Thermodynamic Considerations. Journal of Catalysis 199(2) (2001): 247-258.

[54] Metcalfe, I.S. Electrochemical Promotion of Catalysis: II: The Role of a Stable Spillover Species and Prediction of Reaction Rate Modification. Journal of Catalysis 199(2) (2001): 259-272.

[55] Kokkofitis, C., Karagiannakis, G., and Stoukides, M. Electrochemical promotion in O2− cells during propane oxidation. Topics in Catalysis 44(3) (2007): 361-368.

[56] Papadakis, V.G., Pliangos, C.A., Yentekakis, I.V., Verykios, X.E., and Vayenas, C.G. Improvement of automotive exhaust catalysts by support and electrochemical modification induced promotional effects. Nonlinear Analysis: Theory, Methods & Applications 30(4) (1997): 2353-2361.

[57] Pliangos, C., Yentekakis, I.V., Papadakis, V.G., Vayenas, C.G., and Verykios, X.E. Support-induced promotional effects on the activity of automotive exhaust catalysts: 1. The case of oxidation of light hydrocarbons (C2H4). Applied Catalysis B: Environmental 14(3–4) (1997): 161-173.

[58] Marwood, M., Balomenou, S., Tsiliras, A., Cavalca, C.A., Pliangos, C., and Vayenas, C.G. Electrochemical promotion of electronically isolated and dispersed Pt catalysts. Ionics 4(3-4) (1998): 207-214.

[59] Petrushina, I., Bjerrum, N., Bandur, V., and Cleemann, L. Electrochemical promotion of catalytic reactions with Pt/C (or Pt/Ru/C)//PBI catalysts. Topics in Catalysis 44(3) (2007): 427-434.

[60] Sapountzi, F., Tsampas, M.N., and Vayenas, C.G. Electrocatalysis and electrochemical promotion of CO oxidation in PEM fuel cells: the role of oxygen crossover. Topics in Catalysis 44(3) (2007): 461-468.

[61] Jiménez, V., et al. Electrochemical promotion of the CO2 hydrogenation reaction on composite Ni or Ru impregnated carbon nanofiber catalyst-electrodes deposited on YSZ. Applied Catalysis B: Environmental 107(1–2) (2011): 210-220.

[62] Kambolis, A., et al. Electrochemical promotion of catalysis with highly dispersed Pt nanoparticles. Electrochemistry Communications 19(0) (2012): 5-8.

[63] Balomenou, S., et al. Electrochemical promotion of Pd, Fe and distributed Pt catalyst-electrodes. Solid State Ionics 136–137(0) (2000): 857-862.

[64] Pliangos, C., Raptis, C., Bolzonella, I., Comninellis, C., and Vayenas, C.G. Electrochemical promotion of conventional and bipolar reactor configurations for NO reduction. Ionics 8(5-6) (2002): 372-382.

[65] Poulidi, D., Mather, G.C., and Metcalfe, I.S. Wireless electrochemical modification of catalytic activity on a mixed protonic–electronic conductor. Solid State Ionics 178(7–10) (2007): 675-680.

[66] Poulidi, D. and Metcalfe, I.S. In situ catalyst activity control in a novel membrane reactor—Reaction driven wireless electrochemical promotion of catalysis. Chemical Engineering Science 65(1) (2010): 446-450.

[67] Schreier, M. and Regalbuto, J.R. A fundamental study of Pt tetraammine impregnation of silica: 1. The electrostatic nature of platinum adsorption. Journal of Catalysis 225(1) (2004): 190-202.

[68] Miller, J.T., Schreier, M., Kropf, A.J., and Regalbuto, J.R. A fundamental study of platinum tetraammine impregnation of silica: 2. The effect of method of preparation, loading, and calcination temperature on (reduced) particle size. Journal of Catalysis 225(1) (2004): 203-212.

[69] Vernoux, P., et al. Ionically Conducting Ceramics as Active Catalyst Supports. Chemical Reviews 113(10) (2013): 8192-8260.

APPENDIX

APPENDIX A

CALCULATION FOR CATALYST PREPARATION

Preparation of catalyst for strong electrostatic adsorption (SEA) method

The chemical used for all the catalysts preparation

- Chloroplatinic acid (38% Pt) ,Aldrich
- Yttria-stabilized zirconia (YSZ) ,Inframat Advanced Material

Determination the support which is YSZ to have surface loading 1000 $m^2 L^{-1}$:

From BET surface area of YSZ powder = 58.5749 $m^2 g^{-1}$

Then, $\frac{1000\ \mathrm{m^2 L^{-1}}}{58.5749\ \mathrm{m^2\ g^{-1}}}$ = 17.072 g L^{-1}

For 50 ml, YSZ required in grams = 17.072 g L^{-1}×(50×10^{-3}) L

= 0.8536 g.

Determination weight of chloroplatinic acid to achieve metal solution at various concentration.

Chloroplatinic acid (38% Pt)

For example, metal solution concentration 300 ppm.

For 50 ml,

Then, Chloroplatinic acid required in grams = $\frac{100\ g \times 300{\times}10^{-3}\ g\ L^{-1}{\times}50{\times}10^{-3} L}{38\ g}$

= 0.0395 g

From ICP showed the concentration of Pt on YSZ = 239.6 mg L^{-1}

Hence, %Pt loading = $\frac{239.6{\times}10^{-3}\ g\ L^{-1}}{(17.072{+}239.6{\times}10^{-3})\ g\ L^{-1}}$×100% = 1.384%

Preparation of catalyst for wet impregnation (WI) method

For YSZ powder;

From BET surface area of YSZ powder = 58.5749 m^2 g^{-1}

Base on %Pt loading equal to SEA method = 1.384%

For 50 ml,

- YSZ required in grams = 17.072 g L^{-1}×(50×10^{-3}) L = 0.8536 g.
- Chloroplatinic acid required in grams

$$= \frac{100\ g \times 239.6\times10^{-3}\ g\ L^{-1}\times50\times10^{-3}L}{38\ g}$$

= 0.0315 g

For YSZ disk;

From BET surface area of YSZ powder = 58.5749 m^2 g^{-1} = 58.5749 × 10^4 cm^2 g^{-1}

Surface area of YSZ disk = 1.912 cm^2

$$\text{Surface loading of platinum} = \frac{239.6\times10^{-3}\ g\ L^{-1}}{(17.072\ \mathrm{g}\ L^{-1})\times(58.5749\times10^{4} cm^2 g^{-1})}$$

= 2.396×10^{-8} g Pt cm^{-2}

Then, Surface area of YSZ disc 1.912 cm^2;

It required platinum = 1.912 cm^2×2.396×10^{-8} g cm^{-2}

= 4.58×10^{-8} g of Pt

$$\text{Therefore, Chloroplatinic acid required in grams} = \frac{100\ g \times 4.58x10^{-8}\ g}{38\ g}$$

= 1.205×10^{-7} g

APPENDIX B

CALCULATION FOR THE RATE ENHANCEMENT RATIO AND FARADAIC EFFICIENCY

Propane oxidation: $C_3H_8 + 5O_2 \rightarrow 3CO_2 + 4H_2O$

Electrochemical propane oxidation: $C_3H_8 + 10O^{2-} \rightarrow 20e- + 3CO_2 + 4H_2O$

The rate enhancement ratio, ρ

$$\rho = \frac{r}{r^o}$$

Where r^o = the catalytic rate at open circuit

r = the electrochemically promoted catalytic rate

The Faradaic efficiency, Λ

$$\Lambda = \frac{(r - r^o)}{(I/nF)}$$

Where I = the applied current

F = Faraday's constant (96 485 C mol-1)

n = the charge of the promotion ion

For example,

Feed gas C_3H_8 6.67 cm^3 min^{-1}, O_2 10 cm^3 min^{-1}, He 56.65 cm^3 min^{-1}

No catalyst (blank) obtain CO_2 concentration 0.033 vol%

At open circuit obtain CO_2 concentration 0.036 vol%

At 200 ºC, 6V. obtain CO_2 concentration 0.041 vol% and current 3×10^{-8} A. (3×10^{-8} C s^{-1})

$$r = \frac{1}{3} \times \frac{\frac{(0.041-0.033)}{100} \times (6.67+10+56.65) cm^3 min^{-1} \times \frac{1\ min}{60\ s.} \times 10^5 Pa}{8314000\ cm^3 Pa\ K^{-1}\ mol^{-1} \times (30+273.15\ K)} = 1.293 \times 10^{-9} \text{ mol } s^{-1}$$

$$r^\circ = \frac{1}{3} \times \frac{\frac{(0.036-0.033)}{100} \times (6.67+10+56.65) cm^3 min^{-1} \times \frac{1\ min}{60\ s.} \times 10^5 Pa}{8314000\ cm^3 Pa\ K^{-1}\ mol^{-1} \times (30+273.15\ K)} = 4.848 \times 10^{-10} \text{ mol } s^{-1}$$

Therefor, $\rho = \frac{r}{r^\circ} = \frac{1.293 \times 10^{-9}}{4.848 \times 10^{-10}} = 2.667$

So, $\Lambda = \frac{(r-r^\circ)}{(I/nF)} = \frac{(1.293 \times 10^{-9} - 4.848 \times 10^{-10} mol\ s^{-1})}{3 \times 10^{-8}\ C\ s^{-1}/(20 \times 96\,485\ \text{C mol}^{-1})} = 51964.692$

APPENDIX C

CALCULATION FOR METAL FOR PROPANE OXIDATION

Propane oxidation: $C_3H_8 + 5O_2 \rightarrow 3CO_2 + 4H_2O$

The propane conversion was calculated as = $\frac{P_{CO_2}}{P_{CO_2}+3P_{C_3H_8}} \times 100\%$

where P_{CO2} are the partial pressures of CO_2

P_{C3H8} are the partial pressures of C_3H_8 in the outlet gas

APPENDIX D

CALCULATION FOR METAL DISPERSION AND ACTIVE SITES

Calculation of the metal dispersion by CO chemisorption is as follow;

%Metal dispersion (%D) = $S_f \times \frac{V_{ads}}{V_g} \times \frac{Mw.}{\%M} \times 100\% \times 100\%$

Where, Sf = stoichiometry factor CO:Pt = 1

Vads = volume adsorbed

Vg = molar volume of gas at STP = 22414 $cm^3\ mol^{-1}$

Mw. = molecular weight of metal = Pt = 195.078 g mol^{-1}

%M = %metal

Vinjet = volume injected = 0.02 cm^3

M = mass of sample

Example: Calculation of the metal dispersion of Pt-YSZ by SEA method

%M = %metal = 1.38%

M = mass of sample = 0.05 g

Peak Number	Area	$1-A_i/Af$	$V_i ads (cm^3\ g^{-1})$
1	0.0053	0.8825	0.3530
2	0.0066	0.8529	0.3412
3	0.0108	0.7598	0.3039
4	0.0236	0.4741	0.1896
5	0.0396	0.1174	0.0470
6	0.0411	0.0834	0.0334
7	0.0430	0.0420	0.0168
8	0.0449	0.0001	0.0000
9	0.0449	0.0000	0.0000
sum			**1.2848**

Then, %Metal dispersion (%D) = $1 \times \frac{1.2848\ cm^3 g^{-1}}{22414\ cm^3 g^{-1}} \times \frac{195.078\ g\ mol^{-1}}{1.38} \times 100\% \times 100\%$

= 80.749 %

Example: Calculation of the metal dispersion of Pt-YSZ by wet impregnation

%M = %metal = 1.38%

M = mass of sample = 0.05 g

Peak Number	Area	1-A_i/Af	$V_i$ads(cm^3 g^{-1})
1	0.0081	0.8193	0.3277
2	0.0185	0.5872	0.2349
3	0.0336	0.2514	0.1006
4	0.0401	0.1049	0.0419
5	0.0448	0.0003	0.0001
6	0.0448	0.0000	0.0000
sum			**0.7052**

Then, %Metal dispersion (%D) = $1 \times \frac{0.7052\ cm^3 g^{-1}}{22414\ cm^3 g^{-1}} \times \frac{195.078\ g\ mol^{-1}}{1.38} \times 100\% \times 100\%$

= 44.347 %

Calculation of the metal active site by CO chemisorption is as follow;

Active site (molecule of Pt active g^{-1}) = $(\frac{\%M \times \%D}{100 \times 100 \times Mw.}) \times (6.02 \times 10^{23}$ molecule $mol^{-1})$

Example: Calculation of the metal dispersion of Pt-YSZ by SEA method

Active site = $\frac{0.05 \times 80.794}{100 \times 100 \times 195.078\ g\ mol^{-1}} \times 6.02 \times 10^{23}$ molecule mol^{-1}

= 1.24664×10^{18} molecule of Pt (grams of catalyst)$^{-1}$

Example: Calculation of the metal dispersion of Pt-YSZ by wet impregnation

Active site = $\frac{0.05 \times 44.347}{100 \times 100 \times 195.078\ g\ mol^{-1}} \times 6.02 \times 10^{23}$ molecule mol^{-1}

= 6.84258×10^{17} molecule of Pt (grams of catalyst)$^{-1}$

APPENDIX E

THE CHARACTERIZATION CATALYST BY XPS TECHNIQUE

X-ray photoelectron spectroscopy (XPS) is a technique for analysing the surface chemistry of a material. The XPS spectra, the blinding energy, full width at half maximum (FWHM) and the composition of Pt catalysts on surface of YSZ disk were performed by using the Kratos Amicus x ray photoelectron spectroscopy. The experiment was operated with the x-ray source at 20 mA and 12 kV, the resolution at 0.1 eV/step and the pass energy of the analyzer was set at 75 eV under pressure approximately 10^{-6} Pa.

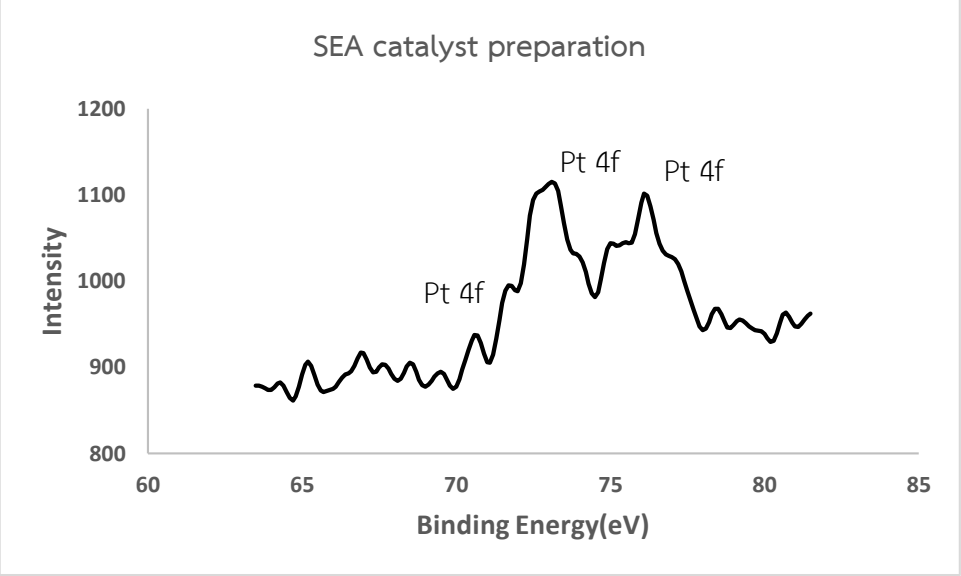

APPENDIX F

CATALYST CHARACTERIZATION BY XRD

The x-ray diffraction (XRD) patterns of the support and catalysts were determined by using the SIXMENS D5000 connected x-ray diffractometer connected to computer with Diffract ZT version 3.3 programs for fully control of XRD analyser. The XRD analysis is conducted to Cu-Kα radiation with Ni filter in the 2θ range between 30° and 130° found only the peak of YSZ. Moreover, it did not have Pt peak for both Pt deposited on YSZ via SEA and WI.

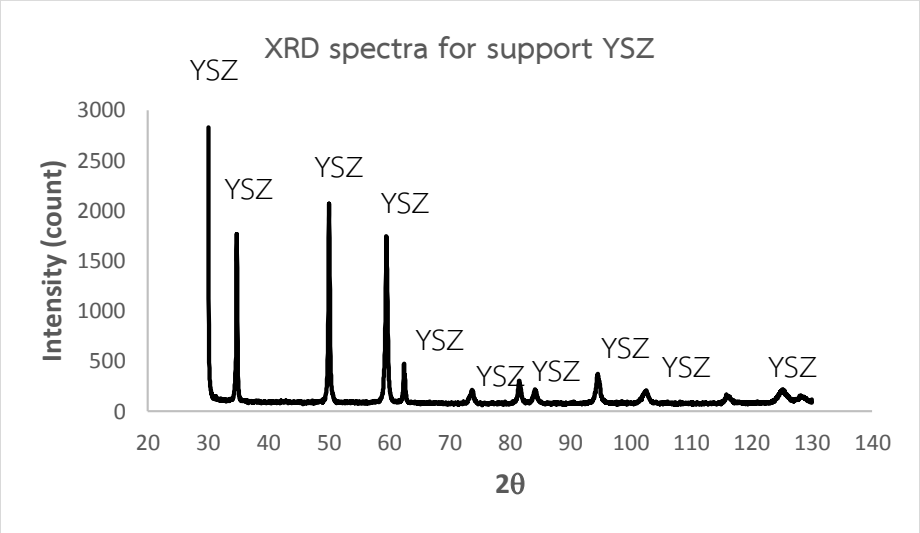

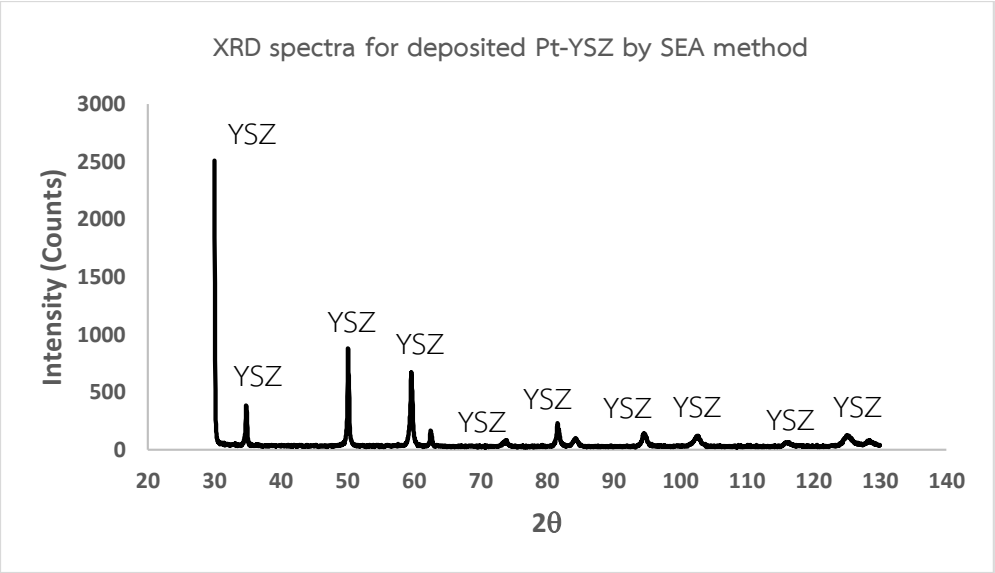
XRD spectra for deposited Pt-YSZ by SEA method
Intensity (Counts)
3000
2500
2000
1500
1000
500
0
YSZ
YSZ
YSZ
YSZ
YSZ
YSZ
YSZ
YSZ
YSZ
YSZ
20 30 40 50 60 70 80 90 100 110 120 130 140
2θ

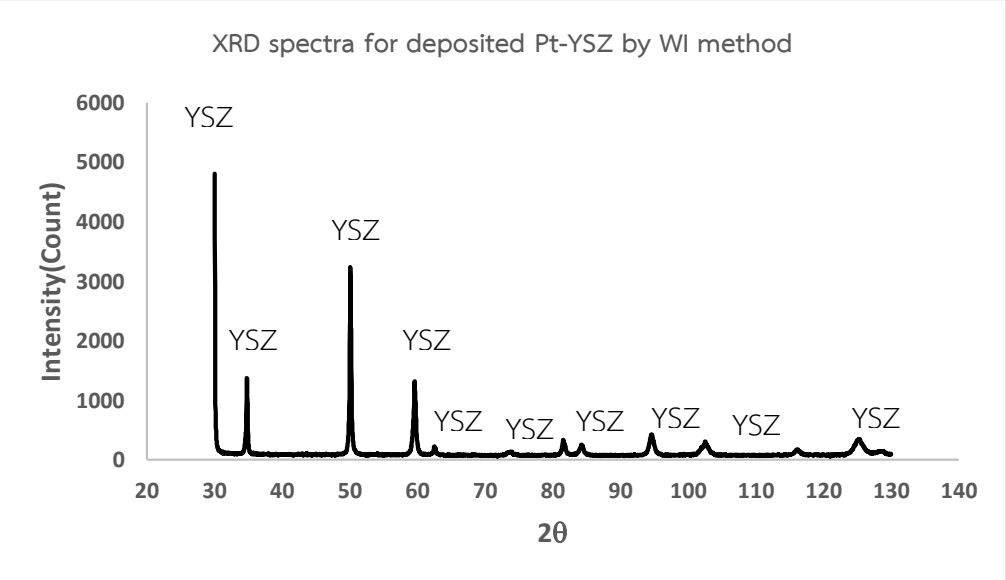
XRD spectra for deposited Pt-YSZ by WI method
Intensity(Count)
6000
5000
4000
3000
2000
1000
0
YSZ
YSZ
YSZ
YSZ
YSZ
YSZ
YSZ
YSZ
YSZ
YSZ
20 30 40 50 60 70 80 90 100 110 120 130 140
2θ

APPENDIX G

THE CHARACTERIZATION CATALYST BY SEM TECHNIQUE

Scanning Electron Microscopy was used to determine the morphology of Pt-YSZ cell. The JEOL JSM-35 CF scanning electron microscope was operated the back scattering mode at 20 kV at the chemical laboratory of department of Engineering, Chulalongkorn University.

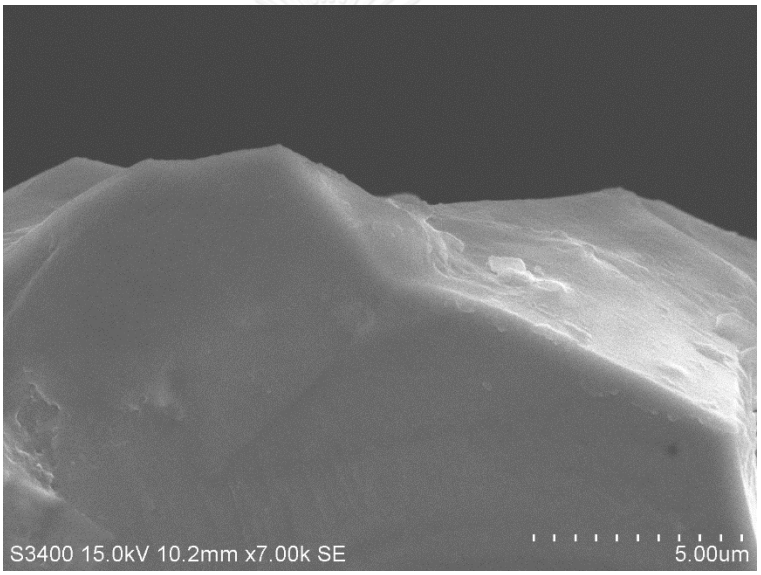

SEM micrograph of YSZ disk

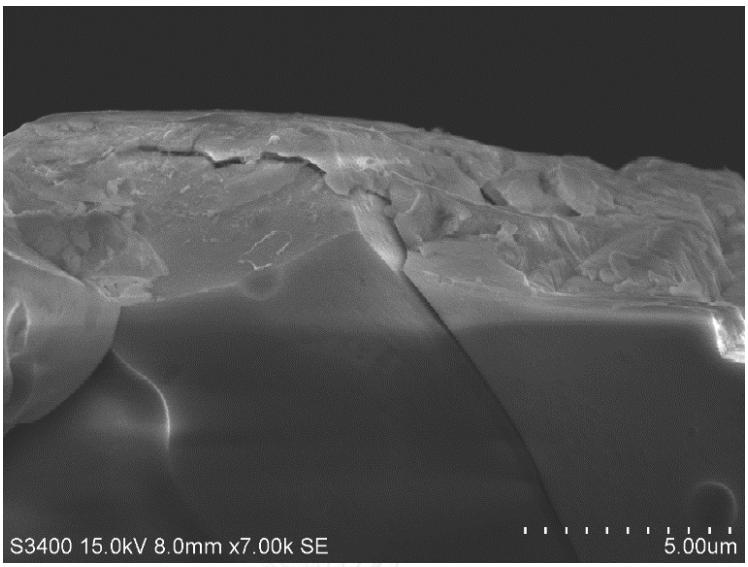

SEM micrograph of a Pt-YSZ cell synthesis by SEA

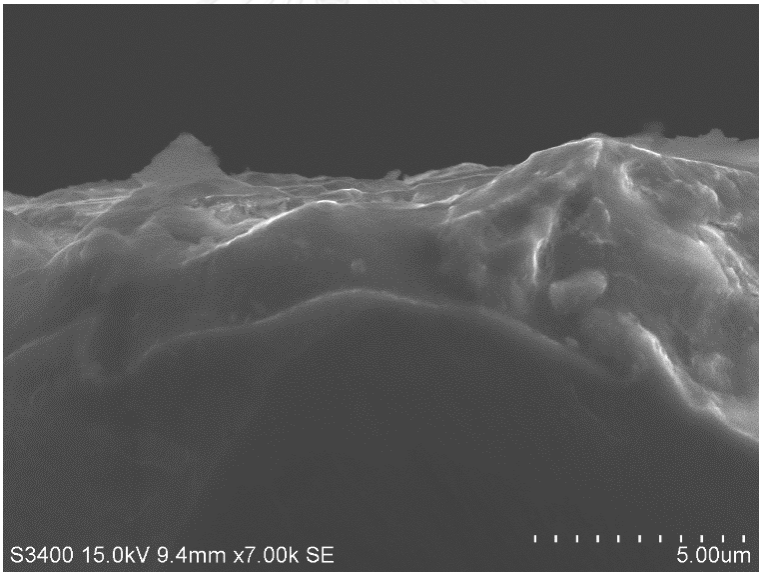

SEM micrograph of a Pt-YSZ cell synthesis by WI

APPENDIX H

THE CHARACTERIZATION CATALYST BY TEM TECHNIQUE

The transmission electron microscope of JEOL JEM-2010 equipped with LaB_6 thermoionic electron gun operating at voltage range of 80-200 kV was employed for TEM analysis.

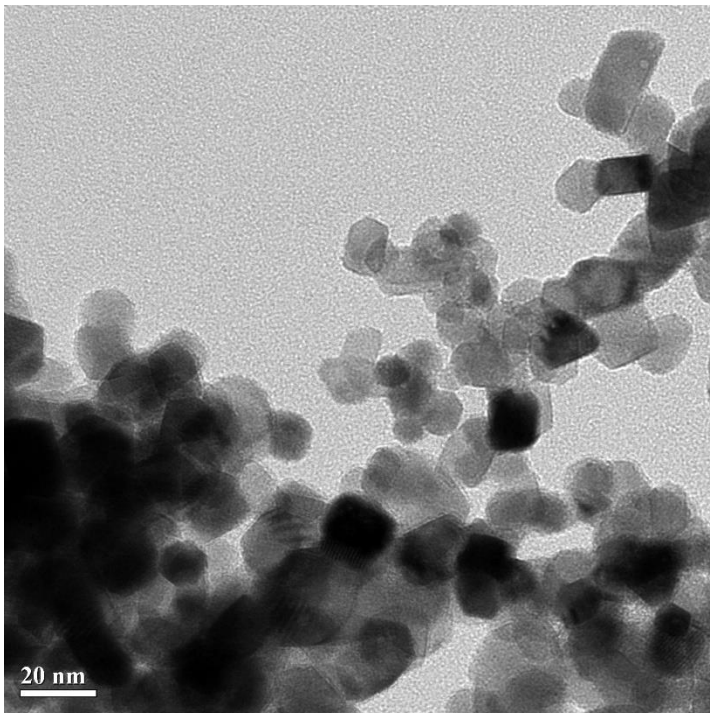

TEM micrograph of a Pt-YSZ powder synthesis by SEA (Pt loading 1.38%)

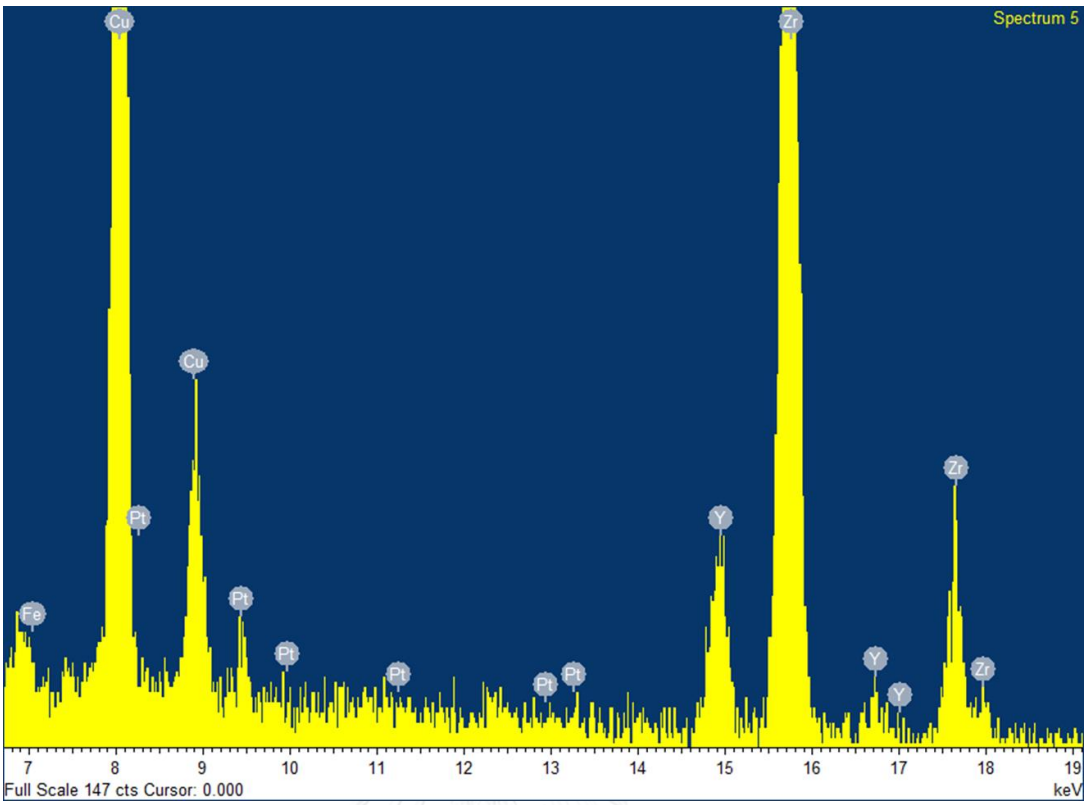

TEM+EDX micrograph of a Pt-YSZ powder synthesis by SEA (Pt loading 1.38%)

VITA

Miss Sopawan Yindee was born on 2 January 1992 in Rayong, Thailand. She received her bachelor degree of Chemical Engineering from Thammasat University, Thailand in May 2014. She continued her master's study at department of Chemical Engineering, Faculty of Engineering, Chulalongkorn University in July 2014.

List of publication:

Sopawan Yindee and Palang Bumroongsakulsawat, "Non-faradaic electrochemical modification of catalytic activity (NEMCA) of propane oxidation on Pt-impregnated YSZ fabricated by strong electrostatic adsorption (SEA)", Proceeding of Pure and Applied Chemistry International Conference 2016, BITEC, Bangkok, Thailand, February 9-11, 2016